AD-A083 492   UNITED TECHNOLOGIES RESEARCH CENTER EAST HARTFORD CONN   F/G 7/4
               CONCEPTUAL DESIGN STUDY FOR COHERENT ANTI-STOKES RAMAN SPECTROS--ETC(U)
               MAR 80   J A SHIRLEY, R J HALL   DAAG46-79-C-0060
UNCLASSIFIED   AMMRC-TR-80-7   NL

END
DATE
FILMED
5 80
DTIC

LEVEL 11 (12) ~ . β

AD

ADA083492

AMMRC - TR 80-7

CONCEPTUAL DESIGN STUDY FOR COHERENT ANTI-STOKES
RAMAN SPECTROSCOPY (CARS) DIAGNOSTICS IN THE AMMRC
BALLISTIC COMPRESSOR FACILITY

MARCH 1980

John A. Shirley and Robert J. Hall
United Technologies Research Center
400 Main Street
E. Hartford, Ct. 06108

DTIC
S ELECTE D
APR 2 4 1980

A

Prepared for

ARMY MATERIALS AND MECHANICS RESEARCH CENTER
Watertown, Massachusetts 02172

DDC FILE COPY

80   4 24 019

AMMRC - TR 80-7

CONCEPTUAL DESIGN STUDY FOR COHERENT ANTI-STOKES
RAMAN SPECTROSCOPY (CARS) DIAGNOSTICS IN THE AMMRC
BALLISTIC COMPRESSOR FACILITY

MARCH 1980

John A. Shirley and Robert J. Hall
United Technologies Research Center
400 Main Street
E. Hartford, Ct. 06108

Final Report Contract Number DAAG46-79-0060

Prepared for

ARMY MATERIALS AND MECHANICS RESEARCH CENTER
Watertown, Massachusetts 02172

REPORT DOCUMENTATION PAGE		READ INSTRUCTIONS BEFORE COMPLETING FORM
1. REPORT NUMBER AMMRC TR80-7	2. GOVT ACCESSION NO.	3. RECIPIENT'S CATALOG NUMBER
4. TITLE (and Subtitle) Conceptual Design Study for Coherent Raman Anti-Stokes Raman Spectroscopy (CARS) Diagnostics in the AMMRC Ballistic Compressor Facility.		5. TYPE OF REPORT & PERIOD COVERED Final Report, July Nov. 1979
		6. PERFORMING ORG. REPORT NUMBER
7. AUTHOR(s) John A. Shirley and Robert J. Hall		8. CONTRACT OR GRANT NUMBER(s) DAAG46-79-0060
9. PERFORMING ORGANIZATION NAME AND ADDRESS United Technologies Research Center E. Hartford, Ct. 06108		10. PROGRAM ELEMENT, PROJECT, TASK AREA & WORK UNIT NUMBERS D/A Project: IL16110EAH42 AMCMS Code: Agency Accession:
11. CONTROLLING OFFICE NAME AND ADDRESS Army Materials and Mechanics Research Center Watertown, Massachusetts 02172		12. REPORT DATE March 1980
		13. NUMBER OF PAGES
14. MONITORING AGENCY NAME & ADDRESS(if different from Controlling Office)		15. SECURITY CLASS. (of this report) Unclassified
		15a. DECLASSIFICATION/DOWNGRADING SCHEDULE

16. DISTRIBUTION STATEMENT (of this Report)

Approved for public release; distribution unlimited.

17. DISTRIBUTION STATEMENT (of the abstract entered in Block 20, if different from Report)

18. SUPPLEMENTARY NOTES

19. KEY WORDS (Continue on reverse side if necessary and identify by block number)

Gas Temperatures	Laser excitation
Rapid determination	CARS
Raman Spectroscopy	Vibrational temperatures

20. ABSTRACT (Continue on reverse side if necessary and identify by block number)

A conceptual design of a diagnostic system using coherent anti-Stokes Raman spectroscopy (CARS) to determine time resolved temperature and species concentrations in the Army Mechanics and Materials Research Center ballistic compressor has been formulated. Performance calculations have been carried out for hydrogen which is an ideal diagnostic species for this application. Results are also presented of computer code calculations of

DD FORM 1473 EDITION OF 1 NOV 65 IS OBSOLETE
1 JAN 73

Block No. 20

ABSTRACT

collision narrowed spectra of nitrogen. Several pump laser systems were compared, and a high repetition frequency Nd:YAG laser was determined to be superior. Population saturation, stimulated Raman gain, and optical breakdown are not expected to pose severe limitations on laser intensity or measurement signal-to-noise ratios. Consideration is given to problems pertinent to operation of the ballistic compressor including compressor recoil, window deflections and generation of CARS from the test section windows. Finally the possiblity of using pulsed stimulated Raman gain spectroscopy (SRGS) as an alternative to CARS at the high densities typical of the ballistic compressor has been identified. SRGS appears to offer adequate measurement ability and possesses certain advantages over CARS.

TR80-7

TABLE OF CONTENTS

i

<u>Conceptual Design Study for Coherent Anti-Stokes
Raman Spectroscopy (CARS) Diagnostics in the
AMMRC Ballistic Compressor Facility</u>

INTRODUCTION

The advent of lasers producing coherent, spectrally pure optical radiation
with electric field strengths on the order of intra-atomic fields has led to a
revolution in spectroscopy. Measurements which previously were unattainable or
impractical have become possible. Diagnostically, the principal advantage of the
laser is the ability to make remote measurements of specific processes with
minimal perturbation of the probed environment. The requirement for making
temperature and species concentration measurements in the AMMRC ballistic compressor
is an application likely to benefit from the emerging, new laser techniques.

Measurements in the AMMRC facility dictate a non-intrusive technique, requiring
minimum optical access, capable of working in the hostile high pressure, high
temperature environment and responding in a fraction of a millisecond. Physical
probes are eliminated from consideration on nearly all these grounds, thereby making
attractive optical techniques which include absorption, fluorescence, Raman scattering
and the nonlinear optical techniques such as coherent anti-Stokes Raman spectroscopy
(CARS). Fluorescence and Raman scattering require a large window aperture and may
suffer interference from background luminosity in certain test mixtures. In addition
fluorescence data might be difficult to interpret because of large quenching rates
particularly at high pressures. Absorption measurements integrate across the line
of sight and hence are of doubtful value in an inhomogeneous medium. Test gas
luminosity poses a potential problem as well for absorption measurements. CARS,
sometimes called degenerate three wave mixing, generates coherent beam-like radiation.
The generated radiation can have intensities of $10^{-2} - 10^{-1}$ W/cm^2, and therefore test
gas luminosity usually poses no problems. CARS is a double ended technique (two port),
and is well suited to the type of optical access available in the AMMRC ballistic
compressor facility. It has the potential advantage over differential techniques,
such as absorption and stimulated Raman gain, in that misalignment of optics due to
vibrations or steering by density gradients such as in a growing boundary layer,
does not produce a signal. In terms of data interpretation the calculation of CARS
spectra at the extreme conditions of ballistic compressor operation appear not to
pose insurmountable problems. Spectroscopic information should permit interpretation
of these data to high temperatures providing Boltzmann equilibrium holds as expected
at these pressures and time scales. The CARS technique thus appears to be the most
promising for ballistic compressor temperature and concentration measurement.

The objective of this investigation was to perform a conceptual study of a CARS system for the measurement of temperature and species concentration in the AMMRC ballistic compressor. The measurement capability of a CARS system using current technology lasers has been assessed and a system design has been formulated which considers the operating characteristics of the ballistic compressor. The evaluation of the CARS system performance for the ballistic compressor is based on the use of hydrogen mixed in the test gas. Hydrogen has a large Raman cross section and simple CARS spectrum making it an ideal thermometric species. It also has the advantage at this time that the extension of CARS signal level predictions to the extreme densities and temperatures attained in the ballistic compressor is fairly straightforward. The CARS signal depends on the spontaneous Raman linewidth. At moderate pressures (1-10 atmospheres) the Raman Q branch transition is pressure broadened. But at high pressure shifting and narrowing has been observed in N_2 and CO. Hydrogen, however, is not expected to collisionally narrow until densities corresponding to several thousand atmospheres at room temperature are reached. CARS spectroscopy in N_2 at pressures to 100 atmospheres is being investigated at UTRC under sponsorship by the Army Research Office. Results of this program should aid the development and verification of calculations in this regime. Calculations have been extended at UTRC to predict the effect of collisional narrowing on the CARS spectra. These are presented herein.

This investigation was divided into an evaluation of the CARS diagnostic capability for the AMMRC ballistic compressor based on H_2 calculations, and the prediction of the effect of collisional narrowing on the CARS spectra of N_2 and CO at high densities. In Section I the theory of CARS is briefly reviewed. Section II reports the results of the conceptual design study. The diagnostic capability of a CARS system for the ballistic compressor has been evaluated and the system components have been laid out and examined. Several candidate pump laser systems have been considered. The CARS signal-to-noise ratio has been evaluated based on actual state-of-the-art high power gas and solid state visible laser technology. There follows a consideration of processes which ultimately limit laser intensities and thereby the CARS signal-to-noise ratio. Basically these processes are optical breakdown, stimulated Raman gain and population perturbation by the pump laser. The selected laser is shown to operate at levels below these limitations. Practical design problems are addressed next in Section II followed by a description of a CARS system for ballistic compressor diagnostics. A unique system is suggested for making spectrally and temporally resolved CARS measurements. Calculations of collisional narrowing effects on high pressure CARS in nitrogen are discussed in detail in Section III. It is shown briefly in Section IV that stimulated Raman gain spectroscopy should also be applicable to ballistic compressor temperature and concentration measurements. Conclusions are contained in Section V, and the references are in Section VI.

SECTION I

COHERENT ANTI-STOKES RAMAN SPECTROSCOPY

With the stimulus provided by the development of high power lasers, Raman spectroscopy has experienced renewed interest. At the same time, nonlinear optical techniques have been investigated to overcome some of the limitations imposed by small spontaneous Raman cross sections. The limited optical access and possible test gas luminosity of the ballistic compressor are best overcome by use of a coherent optical process. Of the variety of nonlinear processes available to the diagnostician, CARS is the most highly developed and has been practically demonstrated. For these reasons, major focus in the conceptual design of an instrument for ballistic compressor studies was placed on CARS. During the study however, another technique, stimulated Raman gain spectroscopy, also emerged as potentially attractive. Although nominally outside the scope of the study, this technique has been briefly surveyed. It will be discussed subsequently in a later section. In this section, the theory and application of CARS will be briefly reviewed.

Coherent anti-Stokes Raman spectroscopy (CARS) is capable of the diagnostic probing of high interference environments due to its high signal conversion efficiency and coherent signal behavior. CARS signal levels are often orders of magnitude stronger than those produced by spontaneous Raman scattering. Its coherent character means that all of the generated signal can be collected, and over such a small solid angle that collection of interferences is greatly minimized. CARS thus offers signal to interference ratio improvements of many orders of magnitude over spontaneous Raman scattering and appears capable of probing compressed media over a broad operational range.

The theory and application of CARS are well explained in several reviews which have appeared recently (Refs. 1-4). Briefly, as illustrated in Fig. 1, incident laser beams at frequencies ω_1 and ω_2 (often termed the pump and Stokes beams respectively) interact through the third order nonlinear susceptibility of the medium, $\chi^{(3)}_{ijkl}(-\omega_3,\omega_1,\omega_1,-\omega_2)$, to generate a polarization which produces coherent radiation at frequency $\omega_3 = 2\omega_1-\omega_2$. It is for this reason that CARS is often referred to as "three wave mixing". When the frequency difference $(\omega_1-\omega_2)$ is close to the frequency of a Raman active resonance, ω_v, the magnitude of the radiation at ω_3, then at the anti-Stokes frequency relative to ω_1, i.e., at $\omega_1 + \omega_v$, can become very large. Large enough, for example, that with typical experimental arrangements, the CARS signals from room air N_2 or O_2 are readily visible. By third order is meant that the polarization exhibits a cubic dependence on the optical electric field strength. In isotropic media such as gases, the third order susceptibility is actually the lowest order nonlinearity exhibited, i.e., due to symmetry considerations, second order effects are nonexistent. The

FIG. 1

CARS — COHERENT ANTI-STOKES RAMAN SPECTROSCOPY

- APPROACH

- ENERGY LEVEL DIAGRAM

- SPECTRUM

78-02-164-3
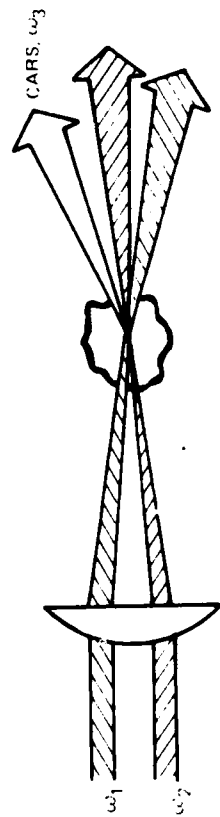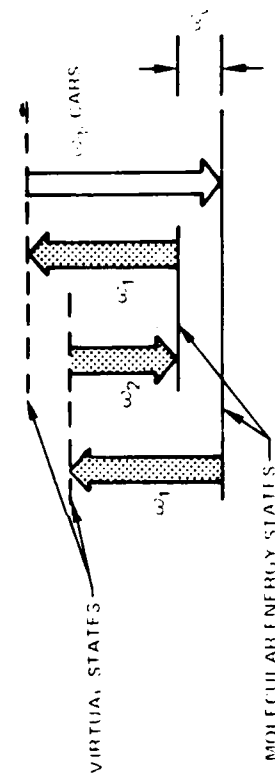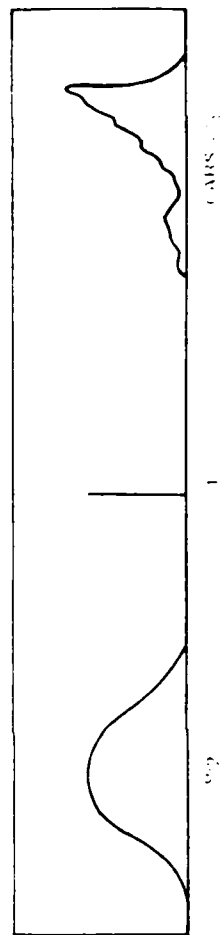
third order nonlinear susceptibility tensor is of fourth rank. The subscripts denote the polarization orientation of the four fields in the order listed parenthetically. In isotropic media, the tensor must be invariant to all spatial symmetry tranformations and the 81 tensor elements reduce to three independent components, χ_{xyyx}, χ_{xyxy} and χ_{xxyy} where $\chi_{xxxx} = \chi_{xyyx} + \chi_{xyxy} + \chi_{xxyy}$. In CARS, which is frequency degenerate, $\chi_{xyxy} = \chi_{xxyy}$ and there are only two independent elements.

Measurement of medium properties are performed from the shape of the spectral signature and/or intensity of the CARS radiation. The CARS spectrum can be generated in either one of two ways. The conventional approach is to employ a narrowband Stokes source which is scanned to generate the CARS spectrum piecewise. This approach provides high spectral resolution and strong signals and eliminates the need for a spectrometer. However, its temporal precision is poor. The alternate approach (Ref. 5) investigated here is to employ a broadband Stokes source as depicted in Fig. 1. This leads to weaker signals but generates the entire CARS spectrum with each pulse permitting in principle instantaneous measurements of medium properties.

For efficient signal generation, the incident beams must be so aligned that the three wave mixing process is properly phased. The general phase-matching diagram for three wave mixing requires that $2\vec{k}_1 = \vec{k}_2 + \vec{k}_3$. $\vec{k}_i$ is the wave vector at frequency ω_i. Since gases are virtually dispersionless, i.e., the refractive index is nearly invariant with frequency, the photon energy conservation condition $\omega_3 = 2\omega_1 - \omega_2$ indicates that phase matching occurs when the input laser beams are aligned parallel or collinear to each other. In many diagnostic circumstances, collinear phase matching leads to poor and ambiguous spatial resolution because the CARS radiation undergoes an integrative growth process. This difficulty is circumvented by employing crossed-beam phase matching, such as BOXCARS (Ref. 6), or a variation thereof (Refs. 7, 8). In these approaches, the pump beam is split into two components which, together with the Stokes beam, are crossed at a point to generate the CARS signal. CARS generation occurs only where all three beams intersect and very high spatial precision is possible.

CARS spectra are more complicated than spontaneous Raman spectra which are an incoherent addition of a multiplicity of transitions. CARS spectra can exhibit constructive and destructive interference effects. Constructive interferences occur from contributions made from neighboring resonances, the strength of the coupling being dependent on the energy separation of the adjacent resonances and on the Raman linewidth which together determine the degree of overlap. Destructive interferences occur when resonant transitions interfere with each other or with the nonresonant background signal contributions of electrons and remote resonances. For most molecules of combustion interest, these effects can be readily handled numerically since the physics describing CARS generation is fairly well understood. At UTRC, CARS computer codes have been developed and validated experimentally for the diatomic molecules, N_2, H_2, CO and O_2 (Ref. 9) and one triatomic H_2O (Ref. 10).

Computer codes are extremely useful for studying the parametric behavior of CARS spectra and, when validated, for actual data reduction.

The CARS intensity I_3 at ω_3 can be expressed as

$$I_3 = \left(\frac{4\pi^2 \omega_3}{c^2}\right)^2 I_1^2 I_2 |\chi|^2 z^2 \tag{1}$$

where I_i is the intensity at frequency ω_i; χ, the third order nonlinear susceptibility, and z, the distance over which the phase matched interaction occurs. The susceptibility can be written in terms of a resonant and nonresonant part, χ^{nr},

$$\chi = \chi' + i\ \chi'' + \chi^{nr}. \tag{2}$$

χ^{nr} is the contribution from electrons and remote resonances. The resonant susceptibility associated with a homogeneously broadened Raman transition, j, is

$$\chi' + i\ \chi'' = \frac{2c^4}{\hbar \omega_2^4} N \Delta_j g_j \left(\frac{\partial\sigma}{\partial\Omega}\right)_j \frac{\omega_j}{\omega_j^2 - (\omega_1 - \omega_2)^2 - i\Gamma_j(\omega_1 - \omega_2)} \tag{3}$$

where $\hbar$ is Planck's constant divided by 2π; N, the total species number density; Δ_j, the population difference between the levels involved in the transition; g_j, strength factor and equal to $(v_j + 1)$ for a Q line; $(\partial\sigma/\partial\Omega)_j$, the Raman cross section for the transition characterized by frequency ω_j; and, Γ_j, the Raman linewidth.

It is quite common in the CARS literature in the case of gases to replace Eq. (1) which is in terms of intensities, with an expression in terms of powers for collinear diffraction limited beams, namely

$$P_3 \propto \left(\frac{\omega_1}{\pi c}\right)^2 \left(\frac{4\pi^2 \omega_3}{c^2}\right)^2 P_1^2 P_2 |\chi|^2 \tag{4}$$

Here the interaction is assumed to occur in a beam diameter, ϕ, and length, ℓ, given by

$$\phi = \frac{4\lambda f}{\pi D} \qquad\qquad \ell = \frac{\pi \phi^2}{2\lambda} \tag{5}$$

where f is the focussing lens focal length; D, the beam diameter at the lens; and λ, the pump laser wavelength. In actuality, most pulsed solid state lasers are not

strictly diffraction limited, but possess divergence angles on the order of 1 milliradian. Nevertheless, Eq. (4) is useful for upper limit estimates of CARS signal levels.

If the detuning frequency, $\Delta\omega_j = \omega_j - (\omega_1 - \omega_2)$ is introduced, the resonant susceptibility may be expressed as

$$\lambda = K_j \frac{\Gamma_j}{2\Delta\omega_j - i\Gamma_j} \tag{6}$$

where

$$K_j = \frac{2c^4}{\hbar\omega_2^4} N\Delta_j g_j \left(\frac{\partial\sigma}{\partial\Omega}\right)_j \frac{1}{\Gamma_j} \tag{7}$$

On resonance $\Delta\omega_j = 0$, and $|\chi| = K_j$. Assuming the CARS beam to have the cross sectional area as the Stokes beam, the CARS power is

$$P_3 = \left(\frac{4\pi^2\omega_3}{c^2}\right)^2 I_1^2 P_2 K_j^2 z^2 \tag{8}$$

The foregoing formulas will be subsequently used to perform signal level estimates for various potential laser sources for the ballistic compressor CARS instrument.

SECTION II

CONCEPTUAL DESIGN OF CARS DIAGNOSTICS FOR THE BALLISTIC COMPRESSOR

In the ballistic compressor, the gas under study is transiently compressed by a free (ballistic) piston driven by gas released from a high pressure reservoir. The test gas is heated nearly adiabatically as the piston is driven down the compressor tube to a high pressure section equipped with windows. Typically pressures in excess of 1000 atmospheres are sustained for 1-2 milliseconds as the test gas is compressed and the motion of the piston is decelerated and reversed. For diatomic test gases, peak temperatures of 2000-4000°K are generated. Because of the polytropic temperature dependence on the compression ratio p/po, the heating time is somewhat longer, i.e. 3-4 milliseconds, than the compression time. The shorter time will be used for estimating the capabilities of CARS diagnostics.

This section addresses the several factors which need be considered in the design of a CARS system for measuring temperature and species concentration in a ballistic compressor. There are a large number of commercially available lasers on the market; suitable types must be identified. In the following section the capabilities of several laser types are determined by estimating the measurement signal-to-noise ratio from laser manufacturer's specifications. Factors which limit the focussed laser intensity are considered and the CARS diagnostic capability within these limitations is estimated. Detectors which are compatible with the envisaged CARS system are then investigated. The section concludes with a description of a CARS system with a general layout and consideration of problems special to the ballistic compressor.

Laser Selection

This section considers the selection of the optimum laser source for CARS diagnostics in a ballistic compressor. Calculations illustrating the tradeoff requirements for selection are developed for the prototypical hydrogen molecular species. Similar calculations can be made for other species such as N_2 and CO. Because of the need to account for collisional narrowing, consideration of these molecules will be left for a latter section of this report. In this section an expression for the signal-to-noise ratio(SNR) for H_2 is derived from the standard CARS power formulation. Next various laser types are considered to assess their applicability to the present problem. Laser vendors have been consulted to obtain specifications of current models and the best performance with state-of-the-art technology. Laser systems considered are summarized in a table on page 11-8.

Several assumptions have been tacitly made in selecting a laser for this application. One is that the Stokes dye laser will be operated broadband to generate simultaneously the entire molecular CARS spectrum. Another is that it is desirable to time resolve the compression pulse. This means that the laser is to be either: (1) cw and modulated by the compression pulse, or (2) pulsed with a time duration long compared to the ballistic compressor pulse or (3) rapidly pulsed. Furthermore, collinear focussing of the beams into the ballistic compressor test section has been assumed. This will give adequate spatial resolution for low f numbers. Candidate lasers for all these modes of operation have been considered.

Hydrogen appears to be an ideal thermometric species for CARS diagnostics at high pressures. The large rotation-vibration interaction in hydrogen splits the lowest vibrational transition into a series of well resolved components. In CARS nearby transitions are coupled together, but the large spacing in hydrogen effectively removes the coupling simplifying the analysis of spectra. The width of the rotational components broaden with increasing pressure because of the effects of rotationally inelastic collisions. Collisional narrowing becomes important when the width of the rotational components becomes comparable to the spacing between components; but because of the large spacing in H_2, collisional narrowing is not expected to be important below a pressure of several thousand atmospheres (Ref. 11). This also considerably simplifies experimental analysis. An additional advantage of H_2 is that it has a relatively large spontaneous Raman cross section for a diatomic molecule, and this leads to relatively high CARS signal conversion efficiency.

In order to compare different candidate laser systems for the ballistic compressor, an expression for the CARS SNR must be derived that is explicit with respect to the pump laser frequency. The formulation for the CARS power, Eq. (6) is repeated here for convenience.

$$P_3 \approx \left(\frac{\omega_1}{\pi c}\right)^2 \left(\frac{4\pi^2 \omega_3}{c^2}\right)^2 P_1^2 P_2 \, |\chi|^2 \tag{9}$$

To reiterate, this expression is appropriate for focussed, diffraction-limited collinear beams. On resonance $\Delta \omega_j = 0$ and

$$|\chi| = K_j = \frac{2c^3}{h\omega_2^4}\left(\frac{d\sigma}{d\Omega}\right)\frac{\Delta N_{vj}}{\Delta k_j} \tag{10}$$

where $\Delta k_j = \frac{\Gamma}{2\pi c}$ is the spontaneous Raman linewidth in wavenumbers, cm^{-1} and $\chi_{VJ} = N\Delta_j$. There is no frequency dependence in the susceptibility, because $d\sigma/d\Omega) \div \omega_2^4$ is a constant (Ref. 12).

The CARS spectrum of H_2 can be simply calculated from the population distribution. The population difference $\Delta N_{VJ} = N_{VJ} - N'_{VJ}$ (for Q-branch transitions) is (Ref. 13)

$$\Delta N_{VJ} = N \, g_J \, \frac{hcB_V\kappa}{kTQ_V} \left\{ \exp \left[-B_V J(J+1) \, \frac{hc}{kT} \right] \right.$$
$$\left. - \exp \left[-B_V' J(J+1) \, \frac{hc}{kT} - \frac{hc\omega_V}{kT} \right] \right\} \tag{11}$$

where g_J is the nuclear statistical weight, B_V is the rotational constant for level v, κ is the symmetry number ($\kappa=1$ for unsymmetric diatomic molecules and $\kappa=2$ for symmetric diatomic molecules), Q_V is the vibrational partition function, ω_V is the vibrational spacing between v and v' and the remaining constants have their usual meaning. At the pressures encountered in the ballistic compressor, compressibility in H_2 is not important, so that $N=p/kT$. For H_2 the nuclear statistical weight is

$$g_J = 1/4, \quad J \text{ even} \tag{12}$$
$$= 3/4, \quad J \text{ odd}$$

The population differences ΔN_{VJ} for $J=0,1,\ldots 7$ are shown in Figure 2 as a function of temperature for p=1000 atm. The odd rotational transitions predominate over the even transitions due to the statistical weighting. There is a shift in population to higher J at higher temperature. This fact can be expolited to determine temperature from CARS spectra as shown in Fig. 3.

The spontaneous Raman linewidth Δk_j for H_2 is pressure broadened at these densities

$$\Delta k_j = B\rho \tag{13}$$

where B is the broadening coefficient, usually expressed in cm^{-1}/amagat and ρ is the gas density (the density in amagats is the ratio of the density of the gas to the density of the gas at one standard atmosphere and $0^\circ C$). For hydrogen $B=1.4\times10^{-3}cm^{-1}$/amagat for Q(1) (Ref. 14).

The signal to noise ratio (SNR) in CARS is frequently limited by shot noise. The photo-detector obeys Poisson statistics (Ref. 15) so that if N_e is the mean number : photoelectrons emitted from the photocathode the standard deviation is $N_e^{1/2}$ and the shot noise SNR is $N_e/N_e^{1/2} = N_e^{1/2}$. The number of photoelectrons can be related to the CARS signal power P_3 and the pulse duration t_p through the detection quantum efficiency η_Q and the collection efficiency ϵ_c:

FIG. 2

HYDROGEN POPULATION DIFFERENCES AT 1000 ATM, 100% CONCENTRATION

79-11-69-6

II-4

FIG. 3
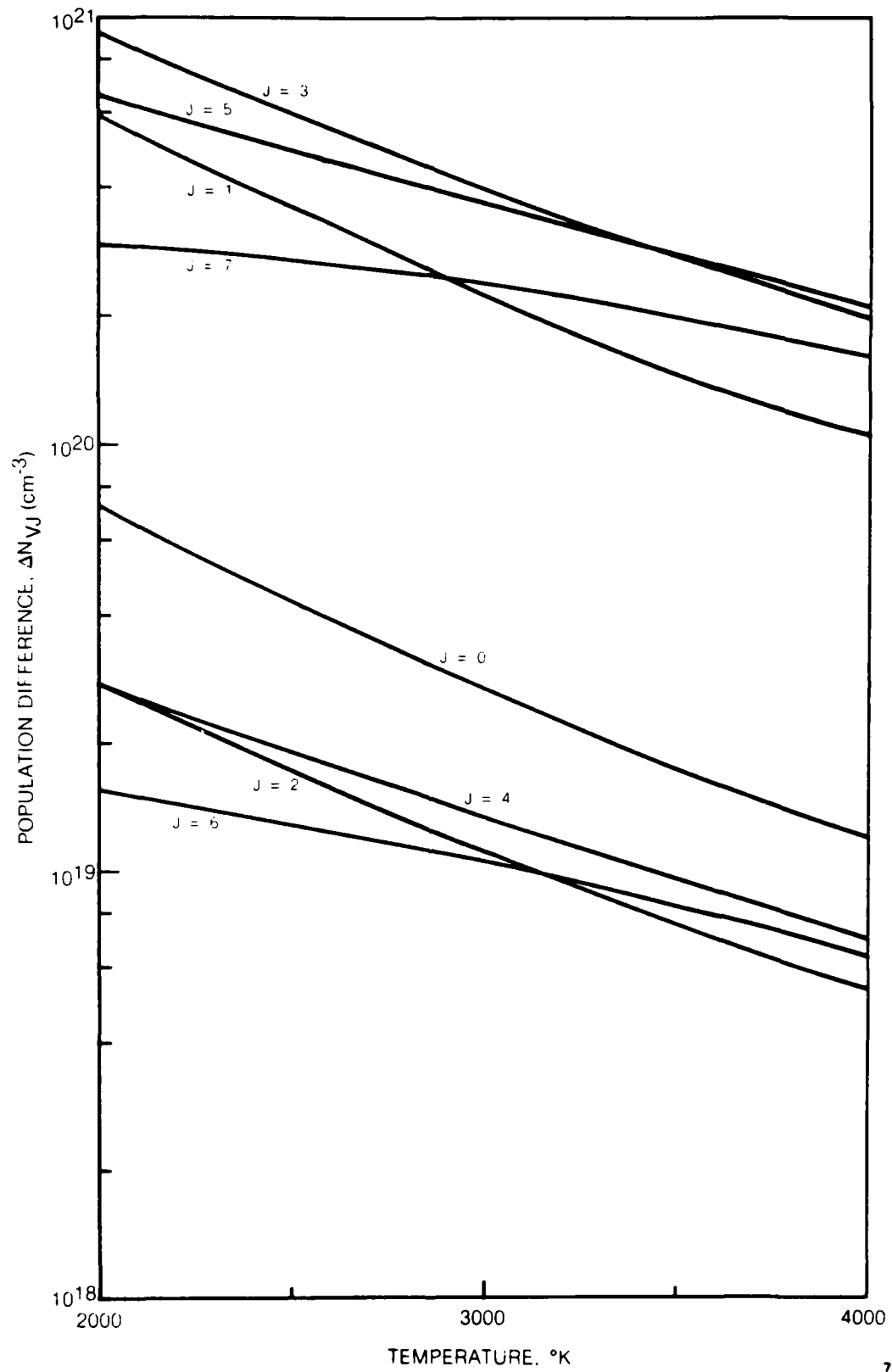
TEMPERATURE VARIATION OF H₂ CARS SPECTRA

1 ATM, 1% H₂, 1 CM⁻¹ SLIT WIDTH

WAVELENGTH — CM⁻¹

79-03-221-7

11-5
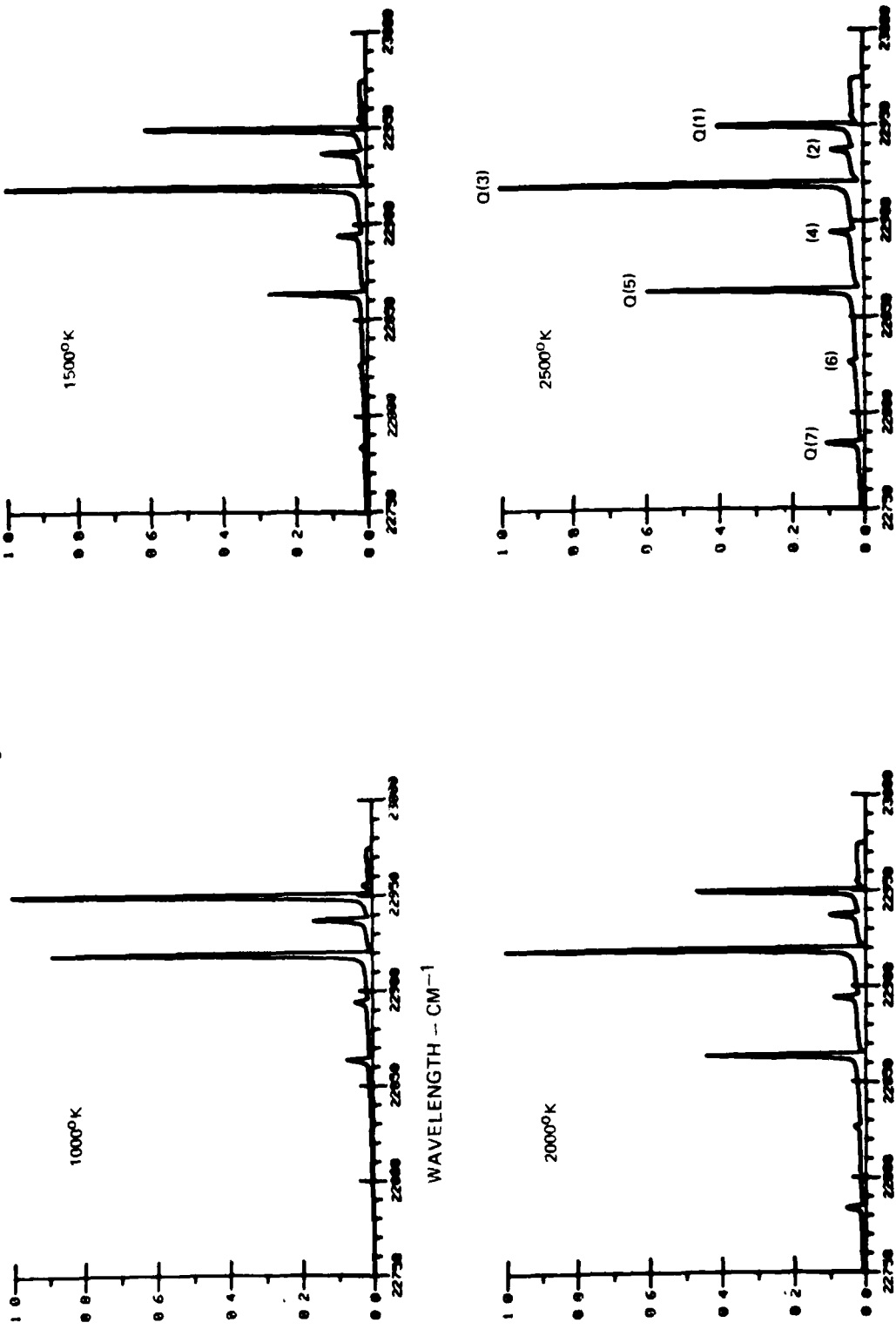
$$SNR = N_e^{1/2} = \sqrt{\frac{n_Q \, \epsilon_c \, P_3 \, t_p}{h\nu_3}} \qquad (14)$$

where $h\nu_3$ is the photon energy. P_3 is given by Eq. (9). It is usual to split off a portion of the primary laser to optically pump the dye laser. If f is the fraction split off then the dye laser power can be written

$$P_D = f\epsilon_D P_L \qquad (15)$$

where ϵ_D is the dye pumping efficiency and P_L is the primary laser power. It is easy to show that f=1/3 for maximum CARS generation. The SNR can then be written

$$SNR \geq A(\lambda) \, P_L \, (P_L t_p)^{1/2} \qquad (16)$$

where $A(\cdot)$ is a constant which depends on the pump laser frequency. The constant $A(\cdot)$ is tabulated in Table I for various lasers. Consideration next will be given to the various laser types suitable for CARS diagnostics.

TABLE I

CARS SIGNAL-TO-NOISE RATIO FOR VARIOUS LASERS

p = 1000 atm, H_2 @ 100% concentration

Laser	$\lambda_{L,}\mathring{A}$	$\lambda_{3,}\mathring{A}$	$A(\lambda), W^{-3/2} sec^{-1/2}$
N_2	3370	2956	6.32
Ar^+	4880	4057	6.47
2xNd:YAG	5320	4356	3.14

The pulsed nitrogen laser radiates in the UV at 3371 $\mathring{A}$. Radiation arises from the second positive system ($C\Pi_u^+ - B^3\Pi_g$) in short (20 nsec) high power pulses. The nitrogen laser appears to be limited to a pulse repetition frequency less than 100 Hz however. In addition the beam quality is usually poor. This can be overcome by using the N_2 laser to drive a dye laser which becomes the pump laser. Because of the low prf the nitrogen laser has not been considered to be viable.

The argon ion laser operates on transitions of the doubly ionized argon atom (Ref. 16). Strong stimulated emission is observed at 4880 and 5145 Å. The CARS frequency dependence favors the 4880 Å line even though the power on 5145 is generally higher. The Ar^+ laser operates continuously with powers up $\sim$10 W on a single wavelength using a prism in the cavity. Since the CARS SNR is proportional to laser power to the 3/2 power and time to the 1/2 power, it is advantageous to use a shorter pulse, higher peak power laser. This can be accomplished with the argon ion laser by cavity-dumping or mode locking. Both techniques use a modulator in the cavity to prevent stimulated emission until a large population inversion is attained, then the modulator is turned on and stimulated emission and laser output rapidly build until the inversion is depleted. Cavity dumpers can be modulated from a few megahertz to single shot. With mode locking the frequency is fixed by the cavity round trip time which is on the order of 91 megahertz. The peak power with either mode locking or cavity dumping is about an order of magnitude higher than the cw power. The pulse duration is typically 200 ns for cavity dumping and 100 ps for mode locked operation. Neither of the leading manufacturers of argon ion lasers offer a cavity dumping option with their highest power models, although both plan to do so in the spring of 1980 (Refs. 17 and 18).

Most other gas lasers have low pulse repetition frequencies, and poor beam quality or lower power. Among solid state lasers, ruby and neodymium-glass are restricted to low prf by the low thermal conductivity in the host material. Yttrium aluminum garnet (YAG), on the other hand, has a good thermal conductivity and therefore when used as a host for neodymium can be used at combined high output power and rep rate.

Nd:YAG emits strong laser radiation at 1.06 μ (Ref. 19) and must be frequency doubled (5320Å) to provide a pump frequency suitable for CARS diagnostics. The Nd:YAG rod is optically pumped with a flashlamp. Several modes of operation are possible depending on whether the flashlamps are cw or pulsed and whether a Q switch is used to increase the peak power. Nd:YAG lasers offered by manufacturers can be divided into: (1) cw flashlamp/Q switched, (2) pulsed flashlamp/Q switched and (3) pulsed flashlamp alone. Typically, pulsed flashlamp models have a prf on the order 1-20 Hz whereas cw flashlamp models can be pulsed at rates up to 10-20 kHz, hence the former have not been considered for this application.

Laser manufacturers have been consulted to obtain specifications consistent with current state-of-the-art technology. The performance of the various laser types is summarized in Table II. The lasers are divided into groups by waveform, and the applicable form of the dependence of SNR on laser power and pulse duration is listed for each waveform group. In this table P_L denotes the peak (or cw) laser power, t_p is the laser pulse duration, and t_m is the measurement time, which is assumed to be a small fraction of the ballistic compression time. For high pulse repetition frequency (f) models, it is assumed that spectra will be averaged over a number of pulses equal to ft_m. The SNR calculated from Equation (16) is shown

II-7

TABLE II
SUMMARY OF LASER SELECTION

* 100% CONCENTRATION H₂

LASER WAVEFORM	SNR FACTOR	TYPICAL LASER	SNR *
(A) CW	$P_1 (P_2 t_m)^{1/2}$	Ar* 7W (cw OUTPUT)	1.23
(B)	$P_1 (P_2 t_m)^{1/2}$	Nd YAG 300W 1.06μ 4W 5320 A (PULSED FLASHLAMP)	0.23 (KDP)
(C)	$P_1 (P_2 t_p)^{1/2}$	Nd YAG P_{PEAK} = 680W t_p = 233 ns f = 10KHz	27
(D)	$P_1 (P_2 t_p t_m f)^{1/2}$	Ar⁺ CAVITY DUMPED P_{PEAK} = 36W t_p = 14ns f = 0.8MHz	1.5
(E)	$P_1 (P_2 t_p t_m f)^{1/2}$	Ar⁺ MODE-LOCKED, SYNCHRO-PUMP DYE P_{PEAK} LASER = 40W, t_p = 100Ps, f = 91MHz P_{PEAK} DYE = 1000W t_p = 2ps	11
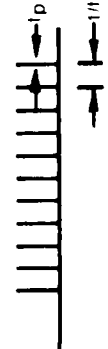
79-11-69-5

in the last column. It represents the signal-to-noise ratio that can be expected
for measurements limited by photon statistics with hydrogen at 100 percent con-
centration, 1000 atmospheres and 4000°K. The value shown represents the minimum
SNR among the first four odd Q branches, i.e. Q(7), and therefore is somewhat
pessimistic. For other Q branches (and other temperatures) the SNR can be
estimated by referring to Fig. 2, and scaling SNR $\sim \Delta N_{vj}$. The SNR values shown
in Table II should be used to compare lasers; realizable measurement SNR's will
be discussed at the conclusion of this section.

One laser type clearly stands out, but it is well to go down the list to
indicate other factors which do not appear in the table. The cw laser approach is
embodied by a high power argon (or krypton) ion laser. The 7 Watts listed represents
a high power model operating with output on a single transition. There appears to
be nothing to be gained by cavity dumping or mode locking. The power is increased
by a factor of five by cavity dumping but the pulse is shortened to 14 nanoseconds
at 0.8 MHz prf. For mode locked operation the peak power is nearly comparable to
cavity dumped operation and the laser pulse decreased to 100 psec. The mode locked
train of pulses are separated by the cavity round trip time (11 nanoseconds), there-
fore the prf is 91 MHz. When the mode locked laser is used to synchronously pump
a dye, it emits a mode locked train of 2-10 picoseconds with a peak power of 1
kilowatt. The pulse time that must be taken in the SNR expression in this case is
the dye laser pulse duration. It is seen that all variants of the Ar^+ laser approach
have similarly low SNR's. Before leaving the argon ion laser it might be noted that
there can be some advantage to using some of the otherwise unused spectral output
of the laser. For example if the 4880Å line is used to provide the CARS pump, the
5145 Å line can be used to drive the dye laser. The scheme increases the predicted
SNR by a factor of 4.5, which is not high enough.

From Table II the high rep rate Nd:YAG laser is predicted to provide the best
performance. The pulsed, non-Q-switched laser can have peak power of approximately
300 W (1 Joule, 3 msec at 1.06 μm) but this power is low for efficient frequency
doubling. The peak power at 5320Å with optimum focussing in the doubling crystal
(Ref. 20) is 4 W with a KDP doubler. With a $LiIO_3$ doubling crystal the conversion
efficiency is much higher, but this crystal has a lower damage threshold. Further-
re it should be pointed out that fixed Q solid state laser are subject to output
iking which would cause measurement problems and may damage the doubling crystal.
he high repetition rate Nd:YAG laser, on the other hand, can have peak powers in
excess of 680 W at 10kHz rate. In these lasers the flashlamp is operated continu-
ously and the Q switch, which is an acousto-optic modulator, is turned on and off
at a high rate by an rf signal. The frequency doubler is placed in the cavity to
increase the doubling efficiency. One possible advantage of these lasers is that
higher laser output power can be obtained at lower prf, so that data rate (or
temporal resolution) can be traded off for improved signal-to-noise. The advantage
of lower rep rate is shown in Table III; which is based on the measured performance
of a recently delivered model (Ref. 21). The SNR shown in this table because it is
for 4000°K and 1000 atm is somewhat pessimistic and does not represent values
achievable under more favorable conditions.

TABLE III

EFFECT OF PULSED REPETITION FREQUENCY ON Nd:YAG ESTIMATED SNR*

f	t_p	P_{peak}	100% SNR
0.5	124	4.5	334
1.0	125	4.6	346
2.0	134	3.7	259
5.0	164	1.9	105
10	233	0.68	27
20	378	0.18	5
kHz	ns	kW	-

* Based on manufacturer's data for a Model 512 QG Control Laser Corp. (Ref. 21).

Laser Intensity Limitations

Up to this point attention has been focussed on maximizing the signal power to maximize the photon statistics-limited signal-to-noise ratio. There are factors which limit the laser intensity in practical applications, however. These are discussed briefly below.

Stimulated Raman Gain

Stimulated Raman gain occurs when the incident pump laser intensity is very high. Amplification is produced at the Stokes frequency with a gain, G such that (Ref. 22)

$$G = \frac{I_\lambda}{I_i} = \exp(g_s I_L \ell) \tag{17}$$

where the gain coefficient g_s is

$$g_s = \frac{16\pi^2 c^2 \Delta N_{VJ} g_j}{\hbar \omega_s^3 n_s^2 \Gamma_j} \left(\frac{d\sigma}{d\Omega}\right)_j \tag{18}$$

where ΔN_{VJ} is the population difference between the Jth rotational sublevel of the vth vibrational state and the next higher vibrational state; Γ_j is the Raman linewidth (radians/sec) and n_s is the index of refraction at the Stokes wavelength. Perturbation of the Stokes wave will be most serious at the highest density compressions. The population difference ΔN_{VJ} was calculated for compressions of 1000, 2000, 3000, 4000 and 5000 with p_o = 1atm assuming an adiabatic polytropic relation

for the temperature (Ref. 23). The maximum ΔN_{VJ} is 3.38×10^{20} for $J = 5$ at $\cdot = 4000\text{-}5000$ atm.

Using this value the gain is calculated to be

$$g_s = 4.3 \times 10^{-10} \frac{cm}{W} \cdot I_L \tag{19}$$

For a focussed beam I_L is a function of distance along the focal axis. The gain was integrated numerically through the compressor test volume by dividing the focal region into 20 regions along the focal axis. The intensity was evaluated for each region for the diffraction limited beams (worst case) according to

$$I(z) = \frac{4P_L}{(f\theta_1)^2} \left[1 + \left(\frac{D_o z}{f^2 \theta_1}\right)^2\right]^{-1} \tag{20}$$

where f is the focal length of the focussing lens, θ_1 is the beam divergence of the laser, D_o is the beam diameter at the lens and z is the coordinate along the focussed beam with $z=0$ at the center. The Nd:YAG laser considered for this application must be beam expanded ($\sim 4x$) to focus the beam to a small diameter. In this case $\theta_1 = 0.5$ milliradian and $D_o = 6$ mm. The gain G integrated across the test volume is then

$$G = \prod_i^{\ell/\Delta z} \exp(g_s I_i \Delta z) \tag{21}$$

where ℓ is the test section length, Δz is the strip width, and $I_i = I(z_i)$. This equation has been evaluated for the parameters above for $f=10$ cm; the results are summarized in Table IV.

TABLE IV

PREDICTED STIMULATED RAMAN GAIN PERTURBATION
Diffraction limited beam, $f=10$ cm

Rep Rate	P_L	G
0.5	4500	1.028
1	4600	1.029
2	3700	1.023
5	1900	1.012
10	680	1.004
kHz	W	–

These calculations show that the Stokes gain is becoming significant at the higher power levels. Since the Stokes gain depends on the quantum level, temperature measurements as well as concentration measurements would be perturbed by this effect. It is important to note that SRG could be used to make temperature and concentration measurements. There are, in fact, certain advantages to doing so; this subject will be taken up in Section IV.

Saturation

The second potential limitation arises from the population perturbation which Taran (Ref. 24) demonstrated can be expressed on line center by

$$\tau_\Delta^{-1} = \frac{1}{\Delta_j} \frac{d\Delta_j}{dt} = 2 \left(\frac{4\pi c}{\hbar\omega_2{}^2}\right)^2 g_J \left(\frac{\partial \sigma}{\partial \Omega}\right)_j \frac{I_1 I_2}{\Gamma_j} \tag{22}$$

where Δ_j is the fractional population difference ($= N_{vj}/N$). Since $\Delta_j(t) = \Delta_j(0)$ exp $(-t/\tau_\Delta)$, the population distribution will not be perturbed if $\tau_\Delta \gg t_p$, where t_p is the laser pulse duration. For broadband Stokes radiation the intensity within the Raman linewidth should be used in this expression. For H_2, assuming $\Gamma_j \approx 0.15$ cm^{-1} (x $2\pi c$) $\tau_\Delta = 1.54 \times 10^{11}$ $(I_1 I_2)^{-1}$ sec where the intensities are in W/cm^2. The Nd:YAG intensity at 10kHz is ≈ 0.30 GW/cm^2. If one assumes the dye intensity is 10 percent of this value and has a spectral bandwidth of 200cm^{-1}, a time constant of 23 msec is calculated, which indeed is much larger than the laser pulse duration. Therefore the Nd:YAG should not seriously perturb the medium at the intensity levels being considered.

Optical Breakdown

The high electric field strength in the focal region of a high power laser can cause the medium being examined to breakdown, that is become fully ionized. Plasma formation substantially alters the medium precluding optical diagnostics. A comprehensive review of laser induced gas breakdown was presented by Smith and Meyerand (Ref. 25). To date most work has been concerned with breakdown at 10.6, 1.06, or 0.6943 μm. In general the breakdown threshold, i.e. the intensity when breakdown becomes highly probable, is a function of laser wavelength, pulse duration, gas pressure and composition. Three pressure domains have been identified as shown in Fig. 4: (1) the low pressure multiphoton ionization regime, (2) an intermediate regime and (3) the high pressure regime in which the collision frequency is greater than the radian frequency of the radiation field. At the pressures of interest in the ballistic compressor the latter case holds and the breakdown threshold increases approximately linearly with the gas pressure. The presence of particulates generally acts to lower the breakdown threshold. Investigators (Refs. 26 and 27) have found that large particulates (i.e. greater than several microns in diameter) decrease clean air thresholds by about two orders of magnitude. Smaller particulates generally have no effect due to the very high electron diffusion

FIG. 4

QUALITATIVE DEPENDENCE OF LASER BREAKDOWN THRESHOLD ON PRESSURE

79-11-69-9
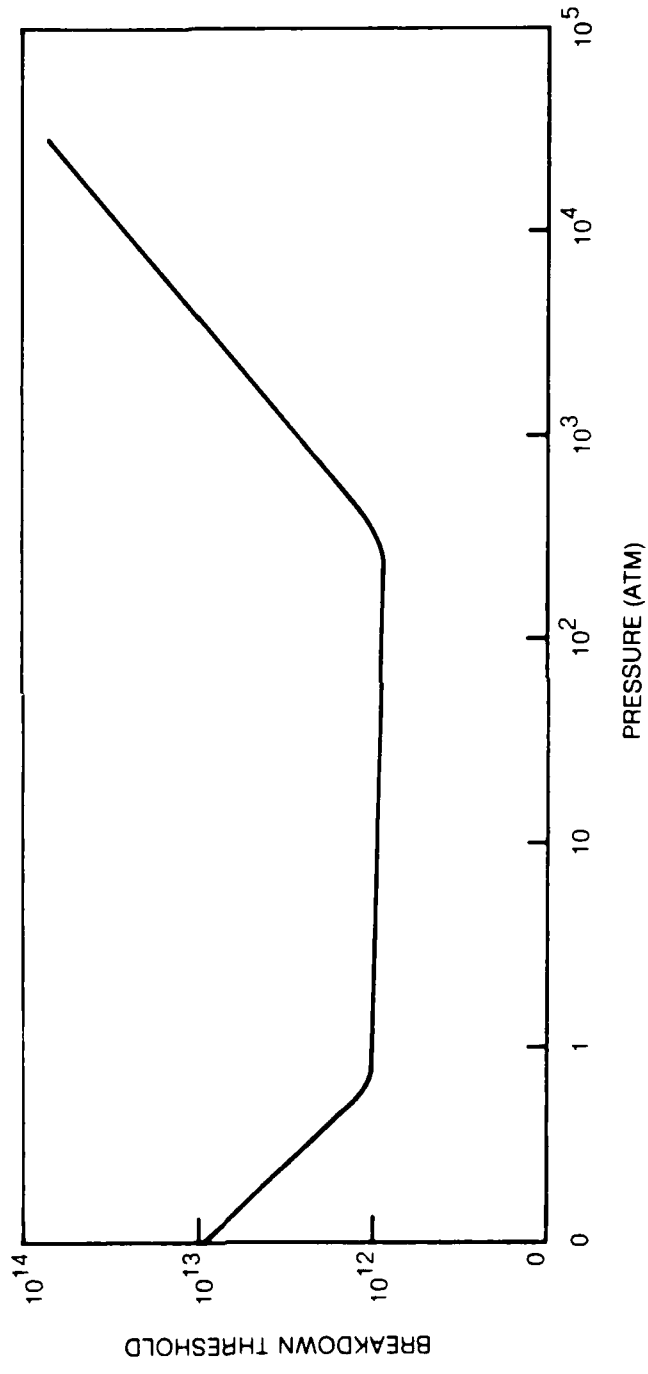
losses. Gas temperatures up to 2000 or 3000°K are generally not expected to affect the threshold level other than through a density effect. In recent experiments in a flame (Ref. 28) this was indeed found to be the case. Furthermore this may also be valid for higher temperatures characteristic of the ballistic compressor because of the low ionization resulting from finite ionization rates.

An estimate can be made of the breakdown threshold. At high pressure the dominant electron energy loss mechanism in nitrogen is electronic excitation at 6.7 eV. Meyerand and Smith (Ref. 25) show that the breakdown intensity is given by

$$I_{Bd} = \frac{800}{p t_p \lambda^2} (1 + 4.5 \times 10^{-6} p^2 \lambda^2) (1 + 2 \times 10^8 t_p p) \tag{23}$$

where the breakdown intensity has units of W/cm^2, wavelength in microns, t_p in seconds and pressure in atmospheres. For a nominal 200 ns pulse of doubled neodymium radiation $I_{Bd} = 1.3 \times 10^{12}$ W/cm^2 at 1000 atm and $I_{Bd} = 1.9 \times 10^{13}$ at 5000 atm. These values are nominally representative of room temperatures. At 3000°K these values are estimated to be: 5.7×10^{11} W/cm^2 (1000 atm) and 7.5×10^{11} W/cm^2 (5000 atm).

The estimated breakdown threshold for clean nitrogen is well in excess of the intensities expected from the Nd:YAG laser. The particles present in the ballistic compressor are not expected to be large enough to substantially affect these estimates, as is also the case when considering H_2 instead of N_2. Therefore optical breakdown is not expected to be a problem in these measurements.

Summary of SNR Calculations

The signal-to-noise ratio for pure H_2 test gas in the ballistic compressor has been estimated for several laser types. The Nd:YAG laser emerges as the most suitable. The cw flashlamp Q-switched type appears to be superior, although a non-Q-switched pulsed flashlamp model may be competitive if predicted doubling efficiency can be sustained with an efficient doubling crystal such as $LiIO_3$. The pulsed flashlamp laser however may exhibit a certain degree of spiking whereas the pulse-to-pulse stability of the Q-switched model is $\pm$ 5%, which should be much better.

Improved SNR performance is predicted for lower repetition rates with the high rep rate YAG because of the higher peak power. Forsaking time resolution entirely and using a single high power pulsed laser such as a pulsed flashlamp, Q switched Nd:YAG laser probably will not gain very much in SNR performance because of the limitation on intensity imposed by stimulated Raman gain. The Stokes gain is estimated to be a few percent for the moderate 300 MW/cm^2 intensity obtainable with high repetition rate lasers. At the intensities that can be reached by the pulsed flashlamp laser ($\sim 10^2$ GW/cm^2) with a 10 cm focal length lens stimulated

Raman gain would preclude CARS measurements. As previously noted SRG could also be used to make measurements in the ballistic compressor. The analysis is somewhat simplified because SRG depends on the imaginary part of the susceptibility. Methods using SRG spectroscopy are discussed further in Section IV.

The SNR results shown in Table III are based on the Q(7) transition which is weaker than the other transitions throughout the temperature range of interest. In general, the more populated rotational states have population differences a factor of 5 higher than Q(7). Since the SNR scales directly with ΔN_{vj} the SNR of the higher populated transitions i.e. Q(3) and Q(5) will be a factor of five larger. Therefore at a repetition rate of 10 kHz the predicted SNR is 135. Thus far signal-to-noise ratio calculations have assumed 100% concentration of H_2. A typical gun barrel composition may contain at most a few percent H_2 depending on the propellant. It is perhaps reasonable to add H_2 up to 10% to the ballistic compressor test gas mixture for diagnostic purposes. The CARS SNR at lower H_2 concentration for the same total pressure depends critically on the magnitude of the foreign gas broadening coefficients. If H_2 is the dominant broadening partner even at low concentration, then the SNR will be proportional to the square root of the hydrogen concentration. On the other hand, if the broadening coefficient of the additive gas is comparable to H_2, then the linewidth will be independent of H_2 concentration and the SNR will scale directly with concentration. Unfortunately the broadening coefficients of other gases such as N_2, CO and CO_2 are not known at the present time. The two limiting cases can be used to bracket the expected SNR range. Taking the lower power Nd:YAG SNR to be 135 at 100% concentration, at 10% concentration one would expect a SNR of 14 for linear scaling and 43 for square root scaling. Measurement accuracies will be considered at the conclusion of this section.

Predictions of CARS measurement capabilities have so far focussed on hydrogen in this section. Nitrogen CARS at high density and pressure is considered explicitly in Section III. The prediction of the spectra is complicated by collisional narrowing. In recent experiments at UTRC very satisfactory agreement between collision narrowed experimental and calculated spectra has been obtained at 100 atm and 300°K. While many more such comparisons will be needed to fully validate the computer model, this initial result appears to be very promising. Because of the narrowing effect the CARS conversion efficiency rises dramatically so that SNR is not expected to be substantially lower for N_2 or like species.

Ballistic Compressor Detection System

The CARS radiation must be spectrally dispersed to make temperature measurements. The dispersed signal can be recorded electronically with a vidicon or a diode array. The vidicon has a photocathode on which light is imaged causing electrons to be accumulated on an adjacent semiconductor surface. An electron beam is scanned over the semiconductor causing a current to flow in an external circuit as charged areas of the film are neutralized by the beam. Operation of the diode array is similar except that the semiconductor surface is replaced by an array of diodes. Currently available vidicons and diode arrays require about 10 milliseconds to scan the detector area. This precludes time resolved CARS measurements in the ballistic compressor in a straightforward manner.

Previously, vidicons for scientific applications were one dimensional. A two dimensional vidicon has recently been introduced i.e. OMA II (Ref. 29). The device can be used to time resolve the dispersed CARS signal by sweeping it across the OMA face. To do this a rotating optical slit is used to permit light to fall successively on different bands along the OMA face. Imagine the OMA face to be a two dimensional surface with x and y axes. Suppose that the CARS spectrum is dispersed along the x axis. If the entrance slit is illuminated with a cylindrical lens that focusses the CARS radiation along the entrance slit, then another slit scanning perpendicular to the entrance slit will permit the dispersed radiation to fall on a strip along the x-axis which sweeps in time across the y-axis. The chopper has many slots and is designed so that there is always an aperture open to the entrance slit. It is in fact designed for a 10 mm slit height. The chopper speed is then set to sweep a single aperture across the entrance slit in a time equal to ballistic compression time. If the laser pulses -10 times per compression time, then 10 strips of dispersed CARS signals will be recorded on the OMA. Timing between the compression and the chopper is not critical. Significant CARS generation may start when the chopper aperture is half way across the entrance slit, then the latter half of the pulse will be displayed on the bottom or top of the OMA depending on the chopper direction. These signals can be manipulated within the detector controller to restore the normal temporal sense to the display. It may be desirable to gate the OMA on at the onset of significant compression to minimize the signal background. Appropriate synchronization can be derived from the magnetic pick-up on the compressor tube. One disadvantage of the rotating optical slit is that most of the CARS signal is blocked by the chopper. This would impose a severe limitation on time resolved CARS measurements at low H_2 concentrations. It may be possible to use a scanning mirror to move the CARS beam focussed by a spherical lens across the entrance slit, thereby avoiding a large attenuation in the signal.

Diagnostic System Considerations

Measurements in the ballistic compressor appear to be a straightforward extension of previous measurements with a few exceptions. The individual components of a CARS system are reviewed in this section. This discussion is followed by the consideration of special problems of ballistic compressor diagnostics such as compressor recoil, window deflections and CARS generation in the windows.

Experimental Arrangement

The CARS diagnostic system for the ballistic compressor is shown schematically in Fig. 5. In this configuration a portion of the doubled output of the Nd:YAG pump laser is split off (1/3 reflection is optimum) to pump a broadband dye laser. The split off beam is directed to a lens L which brings the beam to a focus on the far side of the dye cell DC. This arrangement prevents damage to the glass walls of the cell. Cavity mirrors M are broadband dielectric coated. The aperture A serves to limit the mode volume. Since there are no frequency selective elements in the dye cavity the output is broadband (typically 100-200 cm^{-1}). The dye laser is combined with the pump laser on a dichroic mirror DM coated to transmit the Stokes frequency and reflect the doubled neodymium frequency at 45° orientation. The combined beams are focussed into the high pressure section by lens L and are subsequently collimated by another lens L. Allowance should be made for the effect of the thick windows on the effective focal length of the lens. The beams are dispersed by a Brewster prism (90° deviation prism) and the doubled Nd:YAG and dye beams are trapped. The CARS beam is further filtered with an interference filter (IF) which could also be a cut-off filter. The CARS beam is then focussed onto the entrance slit of the monochromator. A rotating wheel chopper scans the CARS beam across the entrance slit. The monochromator resolves the CARS signal and disperses it onto the face of a two dimensional multichannel analyzer.

A photomultiplier is used in front of the monochromator to collect the CARS signal integrated over all rotational components of the Q branch. This signal can be used to make concentration measurements, but a separate reference leg is required. This is shown in Figure 5 by a beamsplitter reflecting off a portion of the pump and Stokes beams incident on the high pressure test section. The split off beams are sent through a reference cell which contains the same test gas as the ballistic compressor. CARS is generated in this cell, which is maintained at high pressure (500-1000 atm). The reference CARS signal is used to normalize the ballistic compressor CARS signal with respect to laser power fluctuations.

Figure 5 shows a single laser source, but a second laser could be used to drive the dye laser, providing a factor of about 3 increase in the predicted measurement signal-to-noise ratio. The lasers would have a common oscillator driving the Q switch of each laser. To synchronize the optical pulses it would be necessary to provide an adjustable delay between the two lasers. An electronic delay to the Q switch driver is preferable although an optical delay line also is

FIG. 5

SCHEMATIC DIAGRAM OF BALLISTIC COMPRESSOR CARS DIAGNOSTICS

79-11-69-8
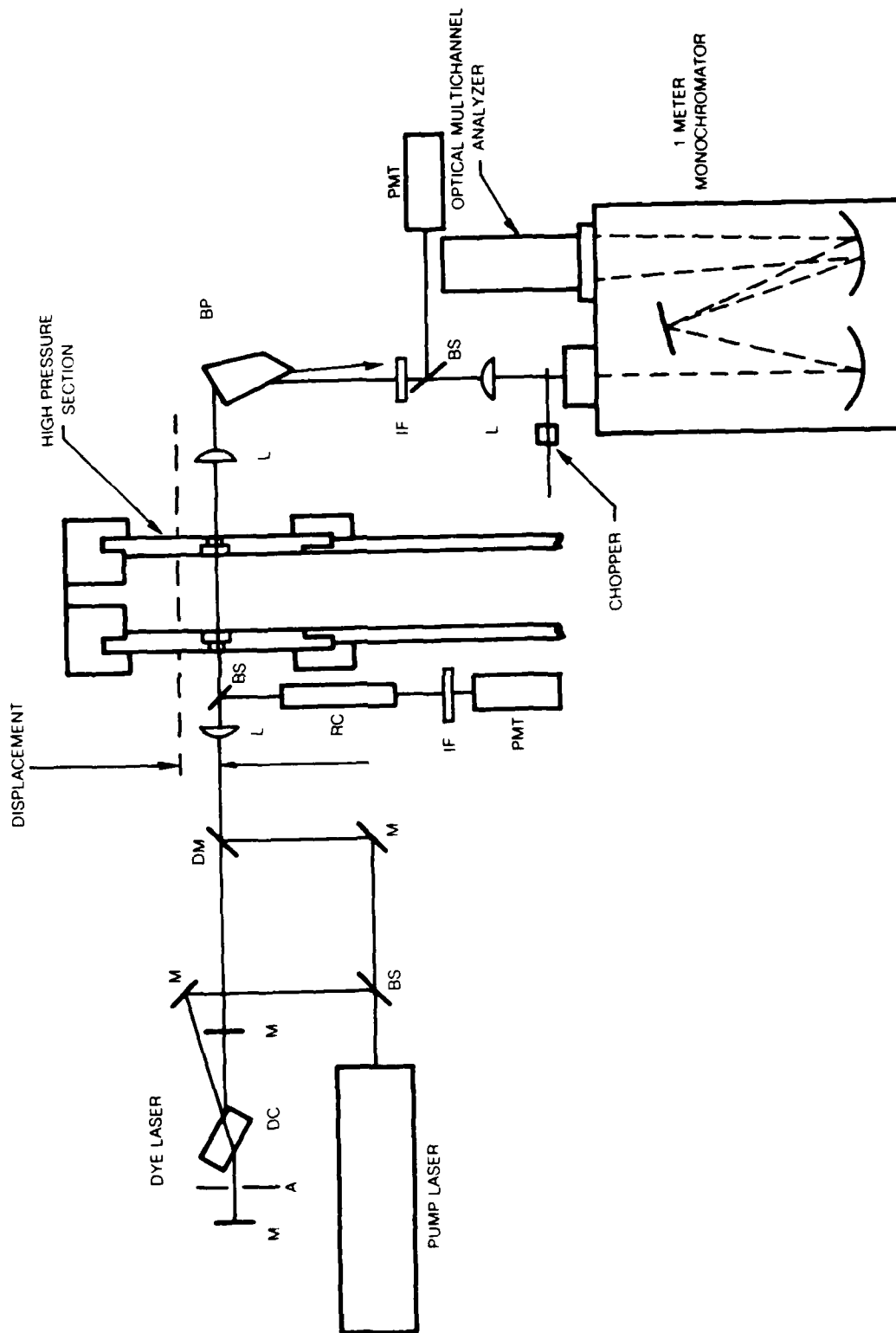
possible. The reason the delay is required is that each Nd:YAG rod has a characteristic time for the build up of stimulated emission after the Q switch is activated. The build-up time in general is different for each rod, but is consistent from pulse-to-pulse for that rod.

Compressor Recoil

When the reservoir pressure is applied to the piston the entire ballistic compressor apparatus moves in a direction opposite to the motion of the piston. The motion is caused by the pressure imbalance between the high pressure reservoir and the low pressure test section. When the piston compresses the test gas to high pressure the pressure imbalance reverses and the motion of the ballistic compressor is momentarily stopped, and reversed. The forces acting on the ballistic compressor when the piston rebounds are relatively high ($\sim$150 g). Designing optics to withstand this acceleration may be possible, but on the other hand the amount of motion is consistent and predictable (typically about 3.6 cm). So it is simpler to align the laser to the axis where the windows are expected to be when the piston rebounds. This approach was adopted by Hammond and co-workers for emission/ absorption measurements (Ref. 23) and should be applicable for CARS diagnostics.

The CARS system can be aligned through the windows prior to firing by translating the entire apparatus which is mounted on sleeve bearings. The laser output can then be prevented by spoiling the Q of the cavity and the ballistic compressor can be moved back to its pre-fire position. When the piston is released and approaches the end of the tube, so that the windows are again aligned with the laser axis, the laser is repetitively Q switched, and the time resolved CARS spectrum is recorded. The approach of the piston can be sensed by the magnetic pick-up mounted on the tube. This signal can be used to gate the laser on, or better, activate an electro-mechanical shutter with the laser operating continuously.

Window Problems

Possible window problems are two-fold. The ballistic compressor windows are highly pressure loaded by the compression tending to form a meniscus lens, thereby possibly distorting the focussed laser beams. The second window problem is that the laser can generate CARS in the window material.

Raman spectra of glasses have been measured by Galeener et. al. (Ref. 30). Fused silica (SiO_2) has a peak cross section at $k=440$ cm^{-1}. There was no structure in SiO_2 beyond about 700 cm^{-1}, nor is any expected. Therefore at the Raman shifts of interest CARS will be generated through the nonresonant susceptibility. Levenson (Ref. 31) determined $\chi_{NR}^{(3)} = 0.7 \times 10^{-7}$ cm^3/J for SiO_2 using two lasers with a difference frequency of 1100 cm^{-1}. Since no structure is expected in this region and beyond to the range of interest for gas diagnostics 1500-4000 cm^{-1}, this value should be reasonable to estimate the CARS generated in the windows. In

this case the intensity formulation must be used (Eqn. 3). With z = 1.27 cm which is the thickness of the window and I_1 = 3.9 x 10^4 W/cm^2 at the window, P_3 is calculated to be 2.9 x 10^{-11}W. This corresponds to a SNR of 1.0 which should be compared with SNR (H_2) = 27 at similar laser power. This level should not cause a problem. There are two approaches that can be taken if window generation were a problem, however. The focal length of the focussing and collimating lens can be shortened thereby increasing the intensity in the gas while lowering the intensity and thereby the CARS generation in the windows. An alternate approach is to generate a reference window CARS level on the detector which could be subtracted electronically later from the test CARS. The background level could be generated at low pressure before the compression. In this case most of the CARS will be generated in the window. CARS generation in the window could be eliminated by a BOXCARS configuration (Ref. 6), but the SNR penalty imposed by the shorter inter-action length precludes its use for this application.

The second window problem that has been examined is bending of the window under the stresses of compression leading to a distortion of the focussed beams. Pressure loading of the window tends to form a meniscus lens. At 3000 atm the deflection at the center of the window is estimated to be 5 x 10^{-5} cm. Assuming the deflected window surfaces are spherical, the focal length of the lens formed by the window is estimated to have a focal length of -7 x 10^5cm (Ref. 32) and therefore should not be a problem.

CARS Measurement Approach for Ballistic Compressor Experiments

Figure 2 shows the effect of temperature on the distribution of the rotational components of the CARS spectrum of H_2. The temperature can be determined from the ratio of the intensities of the more highly populated odd rotational components as measured on the OMA II. The ratios of the intensities can be extracted from the population differences by scaling with $(\Delta N_{VJ})^2$. For other gases, such as N_2 and CO, similar techniques can be used except that the ratio of vibrational bands derived from CARS model calculations must be used. An estimate can be made of the temperature accuracy considering the signal-to-noise ratios for H_2. For a Poisson distribution of photons the temperature uncertainity σ_T is related to the ratio of Q-branch intensities, $r(=N_e/N_e')$:

$$\sigma_T = r\frac{dT}{dr}\left(\frac{1}{N_e} + \frac{1}{N_e'}\right)^{1/2} \tag{24}$$

where N_e and N_e' are the CARS signals (number of cathode photoelectrons of the two levels considered, which can be related to the SNR, i.e. SNR=$N_e^{1/2}$. At 2500°K rdT/dr $\approx$ 1300°K for Q(5) to Q(1) so that with a SNR of about 100 the temperature uncertainty is about 18°K or 0.7%. This is the uncertainty for 100% concentration

hydrogen. At 10% concentration, if the SNR scales as the square root of the concentration, the temperature uncertainty is 58°K. If the SNR scales directly with the concentration the temperature uncertainty is 183°K or 7%. The temperature accuracy can be increased by about a factor of 4 by decreasing the repetition rate from 10kHz to 5kHz, thereby decreasing the temporal resolution as well.

Concentrations can be determined from the integrated CARS intensities, that is the sum of the intensities of the Q(J) lines, which is measured by the PMT looking at the prism dispersed CARS signal in front of the monochromator. To relate the measured signals to the concentration, the effect of laser fluctuations must be accounted for by comparison to the CARS signal generated in the static pressure cell in front of the ballistic compressor test section. The signal can then be related to the concentration if the temperature and linewidth are known. The concentration can be estimated from currently known linewidths for high H_2 concentrations. In order to make precise measurements for equation of state measurements, for example, more linewidth data will be required.

SECTION III

THEORETICAL PREDICTION OF HIGH PRESSURE CARS
SPECTRA OF DIATOMIC GASES

Up to now calculations have addressed ballistic compressor CARS measurements with H_2 thermometric species, because of the simple spectra and lack of collisional narrowing effects. However, nitrogen and carbon monoxide species are more relevant for ballistic compressor experiments. At the extreme densities attained in the ballistic compressor, collisional narrowing is expected to be quite important in these molecules. At moderate pressures, collisions individually broaden the rotational components of the vibrational transitions, which arise from the rotation-vibration interaction. At high density, when the frequency of rotationally inelastic collisions is large compared to the rotation-vibration interaction, a molecule might go through many rotational states during one light scattering process. In this case the molecules would scatter light at an average frequency rather than at the individual rotational-vibrational frequencies. The result is a coalescence of the band to a single narrow peak.

The effect of collisional narrowing on CARS spectra is being studied under an Army Research Office contract. As part of this contract high pressure CARS spectra will be modeled analytically. Results of this analytical effort will be checked with experiments in heated static pressure cells ($p \lesssim 100$ atm, $T \lesssim 1700°K$). Although the corresponding densities are below ballistic compressor values, attempts to understand high pressure AMMRC CARS diagnostics should benefit from the ARO investigations.

Predictions of high pressure N_2 CARS have been made based on the model developed for ARO (Ref. 33). Because CO has very nearly identical molecular constants the predictions are not expected to be greatly different from N_2. Therefore the N_2 results can be taken to be representative of CO within the expected uncertainties.

The theory of high pressure CARS is based on a quantum-mechanical derivation of the third order electric susceptibility that is valid for overlapping spectral lines. Important parameters in the susceptibility expression are the homogeneous, isolated linewidths for all Raman Q-branch transitions, denoted by the symbol Γ. These quantities are the pressure-broadened widths that each transition would have if it were not overlapped by neighboring transitions. At high pressure, adjacent spectral lines will overlap, and it becomes necessary to supplement the isolated linewidths by a matrix of off-diagonal linewidth parameters, denoted by γ, in order to calculate the CARS

spectrum. These off-diagonal elements are related to the rates of collisional energy transfer between molecular states, and govern the collisional, or pressure-induced, narrowing of the CARS signature at high pressure.

All of the calculations to follow assume that N_2 is the active molecule; unless otherwise stated, its assumed concentration is 100 percent. In the numerical calculations, the isolated linewidths Γ_t were assumed to have negligible J dependence and to be given by

$$\Gamma_t = .03 \ p \left(\frac{2000}{T} \right)^{\frac{1}{2}} \quad cm^{-1} \tag{25}$$

for all t where t is an index running over all Q-branch transitions, p is the pressure in atmospheres, and T the temperature in ^{o}K. This simple form is suggested by the measurements of Owyoung (Ref. 34). The off-diagonal linewidth parameters γ_{ts} were calculated from the selection rules $J = \pm \infty$ or ± 2. The density of active molecules N and the background susceptibility χ_{NR} both are assumed to vary simply as p/T. The Stokes laser is assumed to be $200 \ cm^{-1}$ wide, and the combined Gaussian width of the pump and OMA is taken to be $2.8 \ cm^{-1}$.

Pressure-Induced Narrowing

As Fig. 6 shows, collisional narrowing is predicted to play a major role in changing the shape of CARS spectra at the pressures and temperatures of interest in this study.

In examining Fig. 6 it must be appreciated that the widths of the isolated lines are $30 \ cm^{-1}$. Without provision for narrowing, the resulting overlap of transitions leads to a very low resolution spectrum (dotted line) that is devoid of spectral detail. With narrowing, however, a remarkable spectral contraction of each vibrational band occurs, giving rise to distinct 0-1, 1-2, and 2-3 features.

Each distinct vibrational band consists of a large number of neighboring Q-branch transitions. Collisional narrowing causes these adjacent transitions to interfere with each other in such a way that each band contracts, rather than expanding with increasing density.

The width of the 0-1 band at 1000 atm is actually narrower than it is at 1 atm as is shown on Fig. 7. This figure exhibits the calculated pressure dependence of the $2000^{o}K \ N_2$ spectrum for pressure ranging from 1 to 5000 atm. As the pressure increases, the widths of the vibrational bands decrease, at least up to 1000 atm. This is the collisional narrowing effect. At 5000 atm, the bandwidths begin to increase slightly. This is consistent with experimental

FIG. 6

EFFECT OF COLLISIONAL NARROWING ON PREDICTED N₂ CARS SPECTRUM

T = 2000 °K
P = 1000 ATM
Γ_J = 30 cm⁻¹

―――― WITH NARROWING ($\Delta J = \pm 2$)
―― ―― ―― WITHOUT NARROWING

NORMALIZED INTENSITY

FREQUENCY — cm⁻¹

FIG. 7
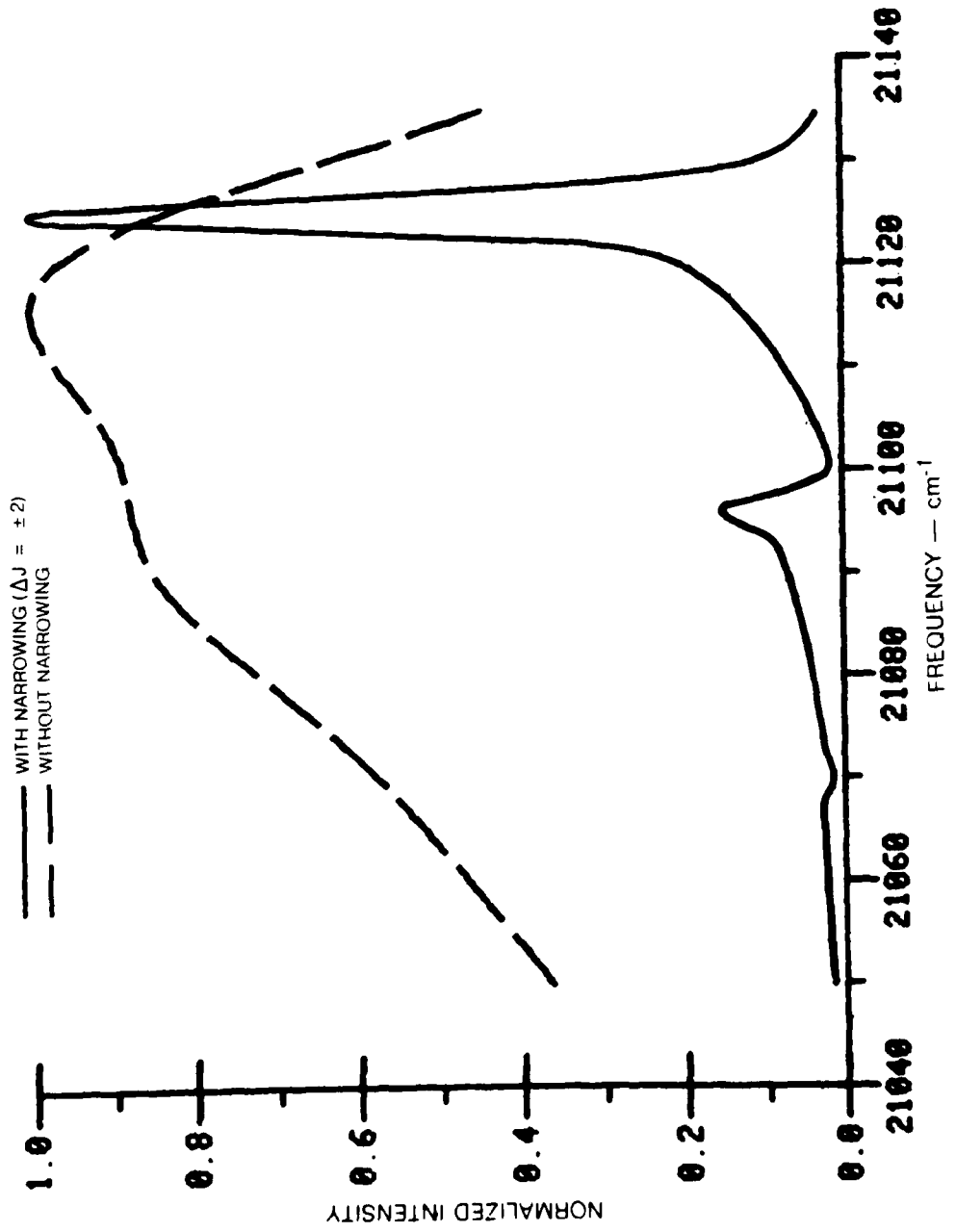
COLLISIONAL NARROWING IN THE CARS SPECTRUM OF N_2

$T = 2000^\circ K$
$\Gamma_J = 0.03 \ CM^{-1} \ ATM^{-1}$
$\Delta J = \pm 2$

79—11—69—4
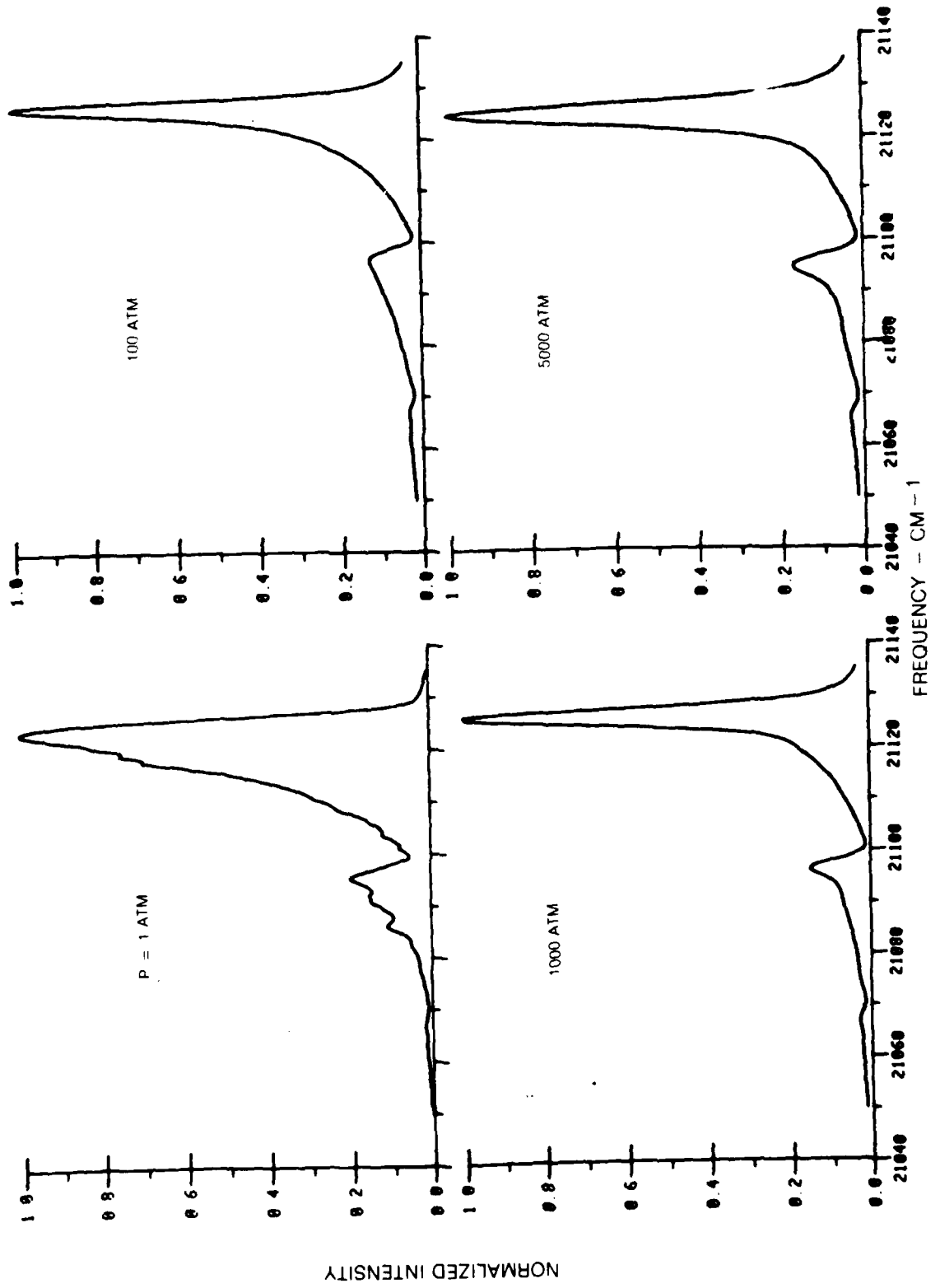
results on the room temperature spontaneous Raman spectrum of N_2 where a leveling off of the width decrease and a slight increase are observed at about 350 amagat (Ref. 35).

The qualitative features of these predicted spectra are sensitive to the model selected for the off-diagonal linewidths, however. Figure 8 shows how the predicted 2000°K, 1000 atm N_2 spectrum changes as the selection rule for the Γ_{ts} changes from $\pm$ 2 to unrestricted. Clearly more will have to be known about these parameters if good theory-experiment fits are to be achieved. It is interesting to see that the $\Delta J = \pm$ 2 selection rule on the Γ_{ts} gives rise to a greater narrowing effect than does the ΔJ unrestricted rule. For the $\Delta J = \pm$ 2 case the coupling terms act over a smaller frequency interval, but the off-diagonal linewidths. $\gamma_{J, J \pm 2}$ are individually stronger than in the case where ΔJ in unrestricted. This fact apparently gives rise to a stronger narrowing effect than is the case for individually smaller off-diagonal elements acting over a larger frequency range.

Thermometry

That CARS will be useful for high pressure thermometry is evident from Fig. 9, where calculated 1000 atm N_2 signatures are shown for T = 2000°K, 3000°K, and 4000°K. It is evident that the 1-2 and 2-3 hot bands are very sensitive to temperature; at 4000°K the strength of the 1-2 hot band actually exceeds that of the 0-1 fundamental. This can occur because the squared matrix elements of the isotropic polarizability are roughly proportional to (v + 1), where v is the vibrational quantum number of the initial state. The ability to perform thermometry will depend on the theoretical prediction that the individual vibrational bands remain sharp. The sharpness of the bands is in turn a consequence of collisional narrowing occuring within each band. If the vibrational dependence of the S matrix is neglected, which should be a good approximation, then transitions belonging to different vibrational bands do not interfere with each other in the narrowing process.

Spectrally Integrated Signals

The spectrally integrated CARS power has also been calculated in each computer run, and the results are shown in Fig. 10 for T = 2000°K. The calculated data points correspond to the signatures shown in Fig. 7. At low pressures it is expected that the integrated intensity will be proportional to pressure (or N). This is borne out by the computer calculations, as can be seen. Actually, the variation between 1 and 10 atmospheres is slightly greater than linear because of the cross-term contributions. At higher pressures, the integrated intensity takes on a pressure dependence that is approximately quadratic ($\sim N^2$). The reason for this dependence is collisional narrowing,

FIG. 8

VARIATION OF PREDICTED N$_2$ CARS SPECTRUM WITH OFF-DIAGONAL LINEWIDTH PARAMETERS
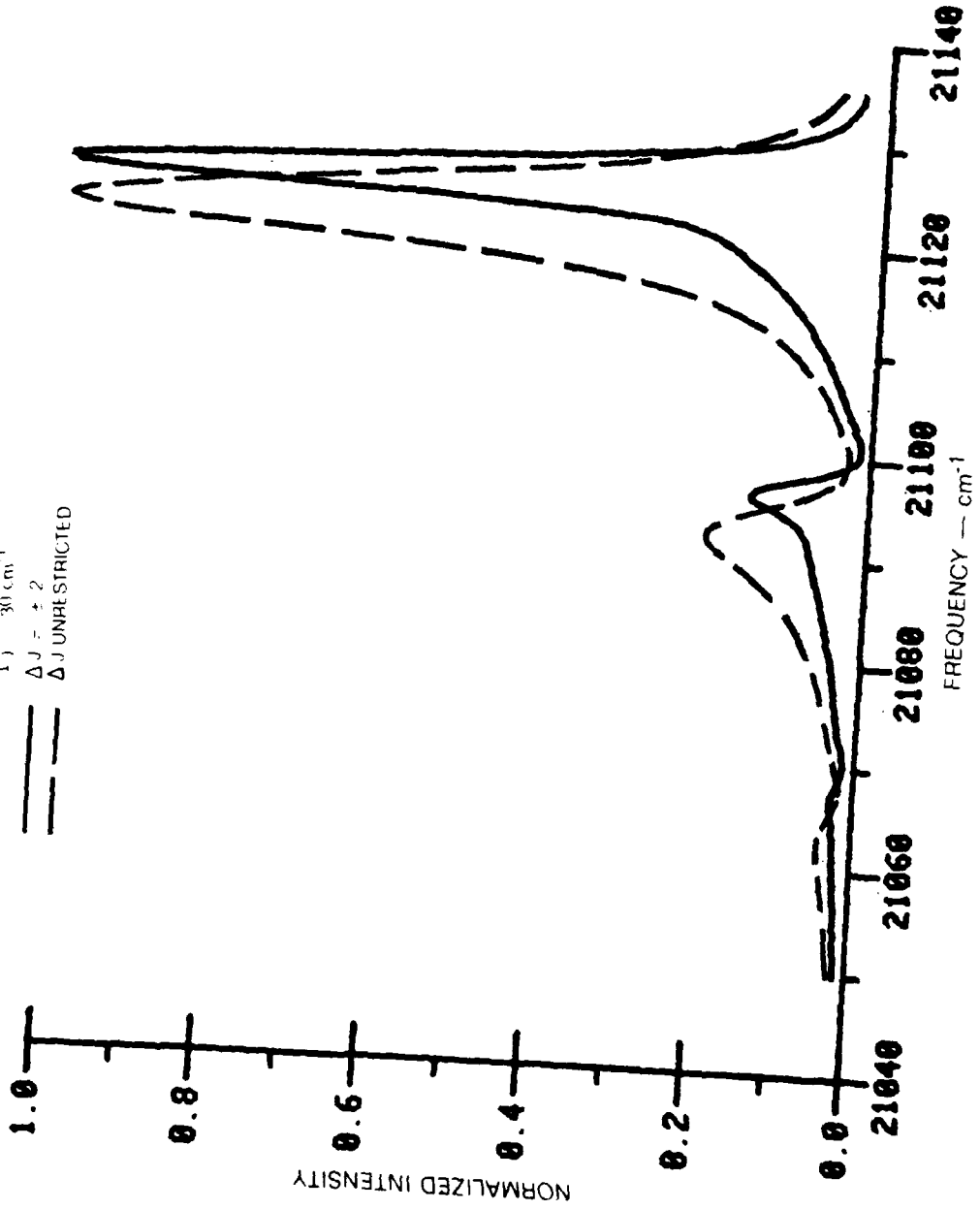
PREDICTED EFFECT OF TEMPERATURE ON HIGH PRESSURE CARS SPECTRUM OF N_2

$$P = 1000 \text{ ATM}$$

$$\Gamma_f = 30 \sqrt{\frac{2000}{T}} \quad CM^{-1} (\Delta J \text{ UNRES})$$
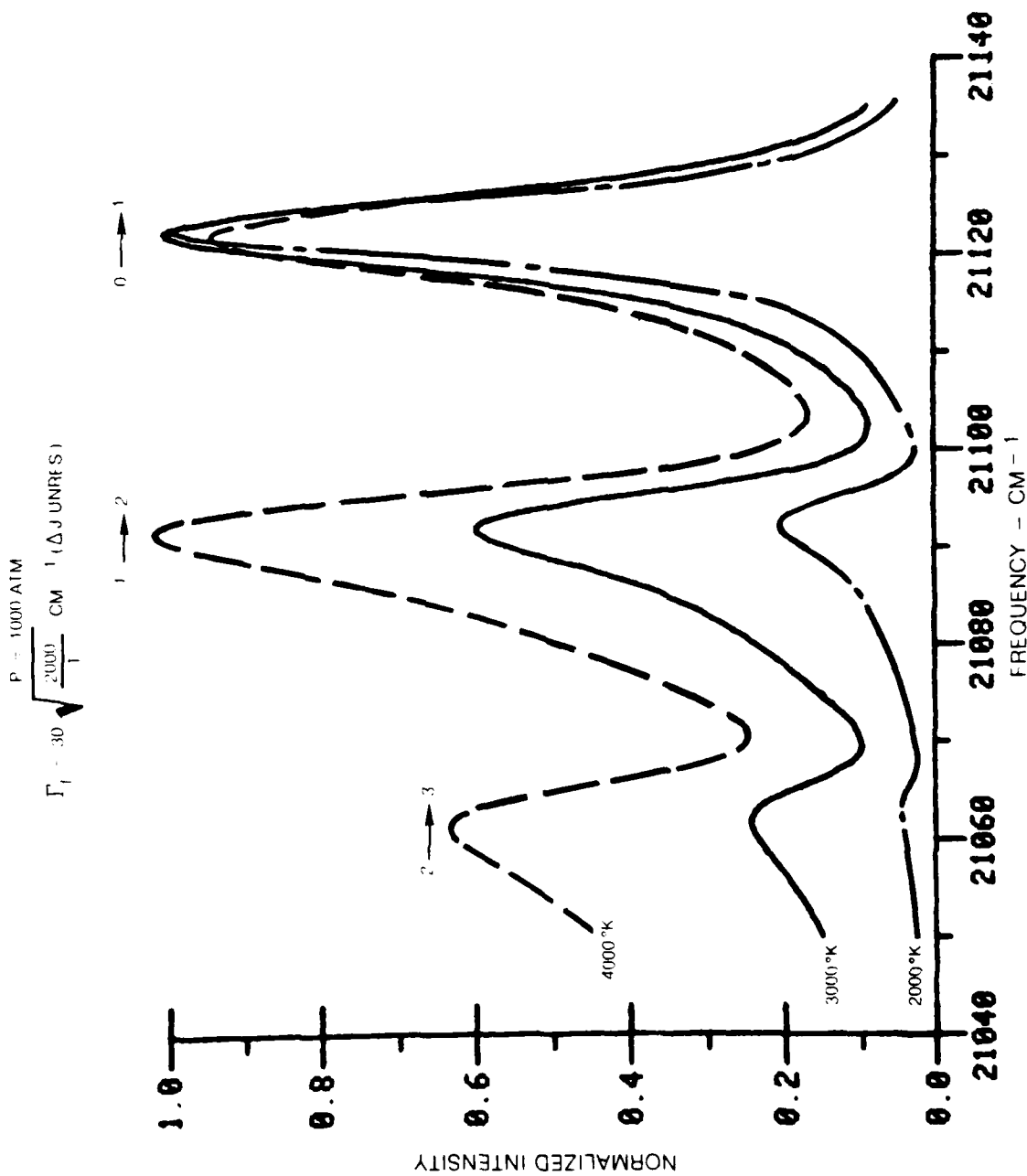
PREDICTED VARIATION OF INTEGRATED CARS INTENSITY WITH PRESSURE

x CALCULATED POINTS FOR
        T = 2000°K
        ΔJ = ±2

79-11-83-3
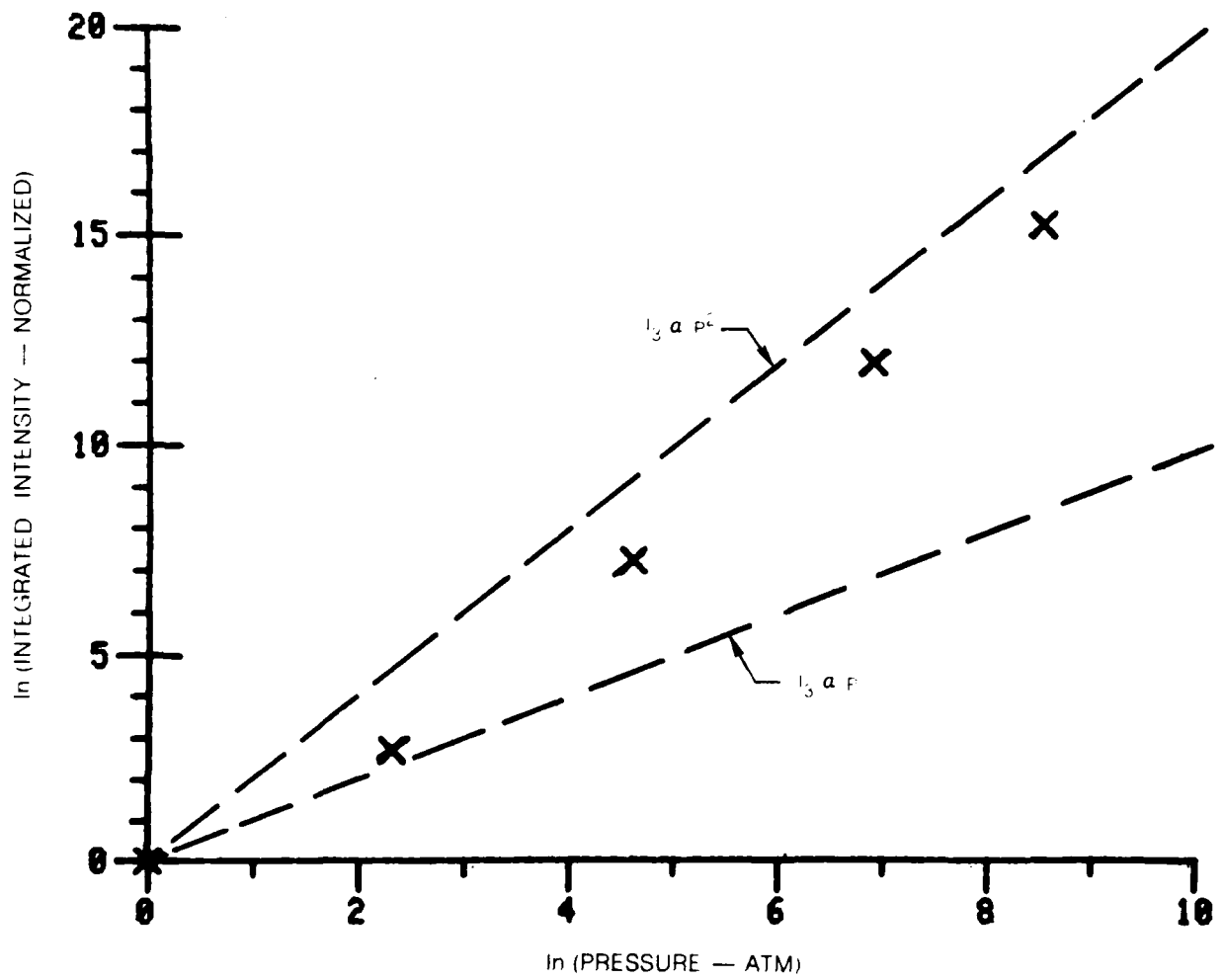
but the explanation for the approximately quadratic dependence is not known. If the 1000 atm calculation is performed without narrowing by setting the $\gamma_{ts} = 0$ (See dotted line, Fig. 6), the integrated intensity is about a factor of 5 lower than the value shown on Fig. 10. The pressure dependence of the predicted $4000^\circ K$ spectra is very similar to that shown in Fig. 10, although the transition from linear to essentially quadratic dependence is slightly less rapid with increasing pressure.

An interesting result is that the calculated integrated spectra do not seem to be very sensitive to the off-diagonal linewidth parameters γ_{ts}, as long as sum rule and detailed balance relationships are observed. For example, changing the selection rule from $\Delta J = \pm 2$ to the unrestricted case results in an integrated intensity variation of less than 2 percent. Changing the energy defect parameter in the $\gamma_{JJ'}$ expression an order of magnitude resulted in an even smaller variation. This result is quite important, for it suggests that density measurements can be derived from the integrated intensity without having to know the off-diagonal linewidths very accurately. However, temperature would have to be first known for this to be feasible.

At a given pressure, the integrated CARS intensity has a strong inverse dependence on temperature as Fig. 11 shows. In part this is due to the trivial fact that the density is varying as $1/T$. Correcting the intensities by dividing by N^2, as Fig. 10 would suggest, does result in a somewhat slower decrease with increasing temperature. This is equivalent to correcting the points for constant density. However, it is apparent that the integrated CARS intensity is not just a function of density, but also has a significant temperature dependence. This means that density cannot be deduced from an integrated intensity measurement alone; information about temperature will also be required.

Minority Species Detectivity

All of the foregoing calculations have been carried out for a mixture of 100 percent N_2. Because there is also interest in CARS for minority species measurement at high pressure, calculations have been carried out for fractional concentrations of N_2 in a background gas having the same background susceptibility as N_2. Figure 12 displays the results of these calculations for 1 percent and 10 percent N_2 at $2000^\circ K$ and 1000 atm total pressure. In each signature the characteristic interference dip at about 21130 cm^{-1} is evident. This dip is caused by destructive interference between the real part of the resonant susceptibility and the background contribution. It is apparent, though, that the situation is very favorable for minority species detection, because the resonant features of the signal are distinct even at 1 percent N_2. This calculation indicates that the detection sensitivity for N_2 is likely to be

CALCULATED TEMPERATURE VARIATION OF INTEGRATED N$_2$ CARS SIGNATURE

P = 1000 ATM
ΔJ UNRESTR
x □ ARE CALCULATED POINTS

FIG. 12
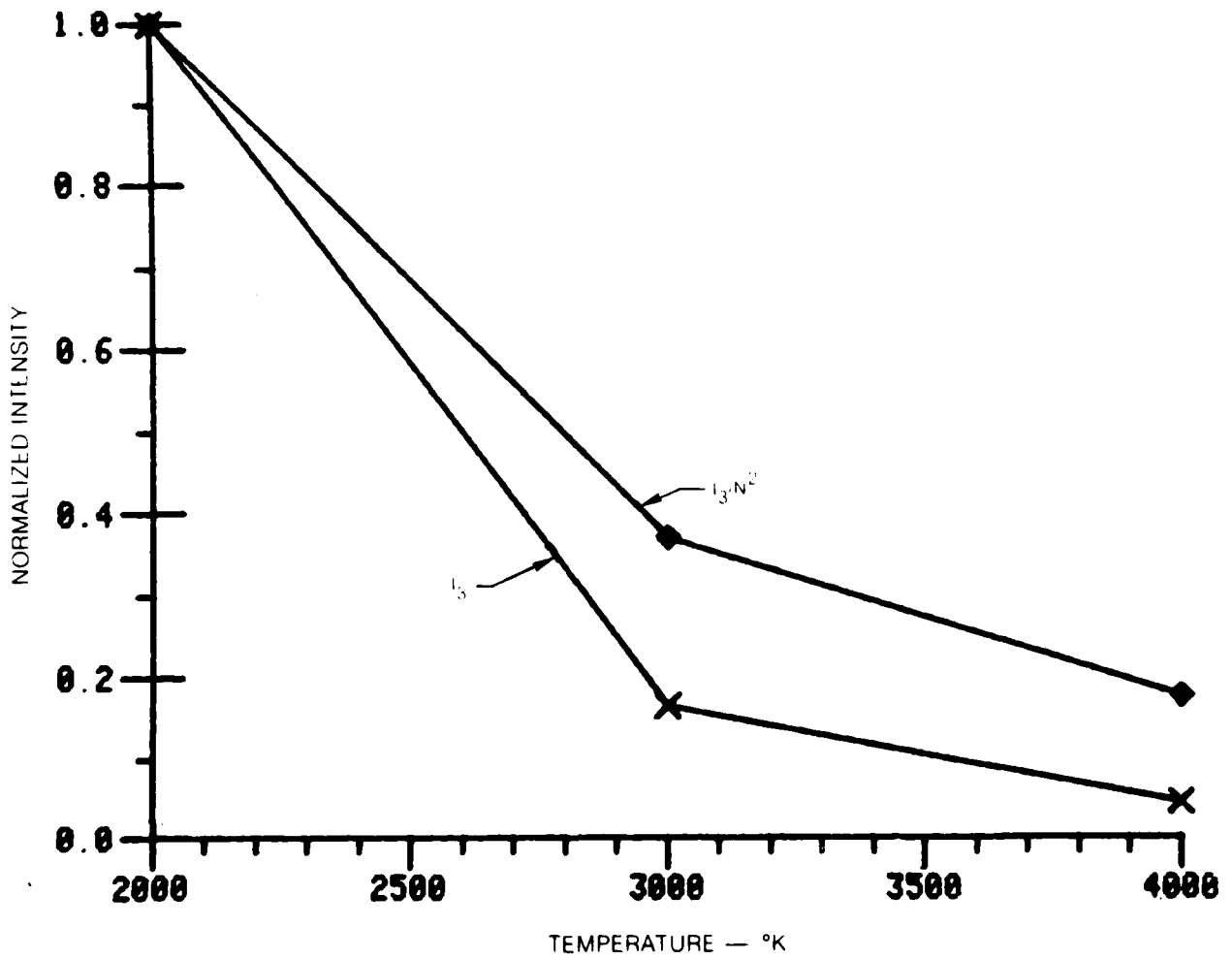
PREDICTED MINORITY SPECIES DETECTIVITY OF HIGH PRESSURE CARS

$$T = 2000°K$$
$$P = 1000 \ ATM$$
$$\Delta J = \pm 2$$

FREQUENCY — cm^{-1}

79-11-83-4

III-11
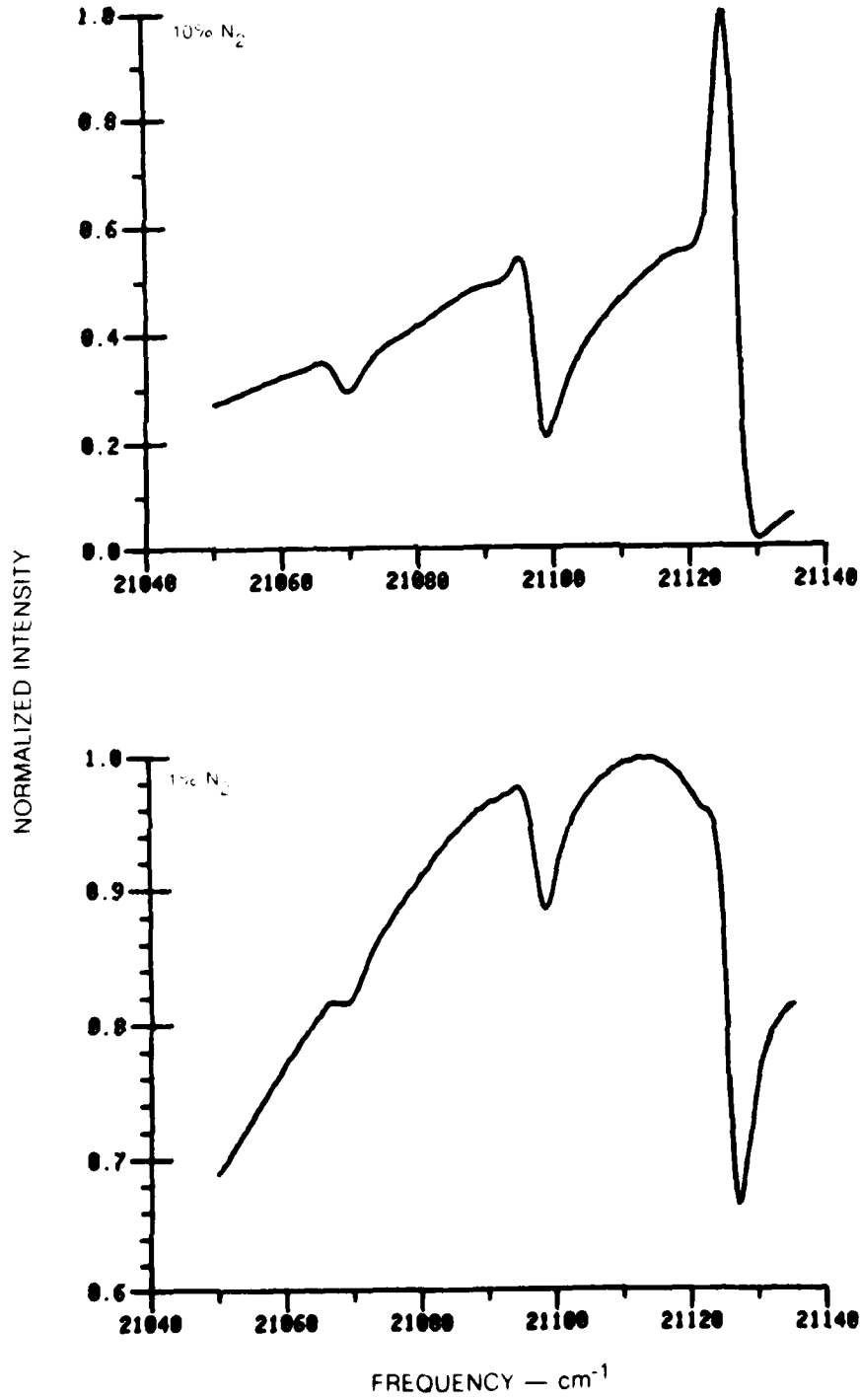
even better than the 1 percent level. There is no reason to expect that the situation will be different for other molecules such as CO, because most of the molecular parameters are similar.

There is an appreciable reduction in CARS power associated with the smaller N_2 concentrations, however. Normalized to the 100 percent N_2 value, the computed 1 percent and 10 percent powers are .018 and .029, respectively. In general we have (Eq. 2)

$$\chi_3 = \chi_R' + i\chi_R'' + \chi_{NR} \tag{26}$$

and the CARS power will be proportional to:

$$|\chi_3|^2 = \chi_R'^2 + \chi_R''^2 + 2\chi_R'\chi_{NR} + \chi_{NR}^2 \tag{27}$$

which for a minority species $|\chi_R| << |\chi_{NR}|$ is given approximately by:

$$|\chi_3|^2 \approx \chi_{NR}^2 (1 + 2 \chi_R'/\chi_{NR}) \tag{28}$$

Summary of Theoretical Analysis and Calculational Results

The theoretical analysis on which these results are based rests on one fundamental assumption, that of the impact approximation. This means that it can be expected to be valid unless the pressure is so high that molecular collisions are no longer of binary type. This means that the collision duration must be appreciably shorter than the mean free path time between collisions. A crude estimate is that this will be satisfied as long as the pressure remains below 10^4 atm at $2000°K$.

In the numerical implementation of the analysis, vibrational dependences of the S-matrix are neglected, making it possible to ignore the line shifts. While there is evidence that this is a reasonable approximation to make, comparisons between experiment and theory at very high pressures may show the need to include these dependences in the theory. In principle, the same analysis used to calculate the isolated linewidths (Eq. 25) could be used to calculate line shifts. In practice, one is only interested in including line shifts if there is a significant dependence of shift on vibrational or rotational quantum numbers.

One of the main results of the computer calculations for N_2 is that the high pressure spectra can be expected to remain qualitatively similar to what is seen at one atmosphere. The large isolated linewidths at pressures on the order of 1000 atmospheres do not totally obscure all spectral detail in the signatures. Due to collisional narrowing, the individual vibrational bands remain relatively sharp. This is very favorable for thermometry, because

temperature can be derived from the relative strengths of these bands. The predicted spectra are, however, sensitive to the off-diagonal linewidth elements, about which little is known at present.

Spectrally integrating the CARS signatures appears to be attractive for making species number density measurements. Interestingly, the predicted integrated intensities don't seem to be sensitive to the selection rules and functional form of the off-diagonal linewidth elements, as long as the collisional narrowing effect is included in the calculations. The integrated intensity is not just a function of density, however, having an appreciable temperature dependence even at constant density. These calculations also show that CARS will be useful for minority species detection at high pressure.

The calculated results presented here represent a large extrapolation from the low pressure calculations that have been found to be in very good agreement with experiment (Ref. 9). At this time, the high-pressure calculations have not been validated because no pertinent experimental data has yet been taken. However, the theory rests on the same quantum-mechanical foundation as analyses of high pressure spontaneous Raman or infrared spectra. The assumptions that have been made are reasonable and consistent with relevant experimental data. We believe, therefore, that there are solid grounds for expecting that experimental high pressure CARS spectra will prove to be similar to what we have presented

here. Recent experiments at UTRC show very satisfactory agreement between calculated and measured spectra under conditions where collision narrowing effects are important. Additional experiments at UTRC, together with further advances in linewidth theory will undoubtedly yield more information about the important off-diagonal elements of the linewidth matrix. The features of the high pressure, high temperature spectra should be such as to make CARS attractive for diagnostics, and it is reasonable to expect that these spectra can be successfully interpreted in terms of parameters that will be well known.

SECTION IV

STIMULATED RAMAN GAIN SPECTROSCOPY

Stimulated Raman gain spectroscopy can be used to make temperature and species concentration measurements. At the high densities attained by the ballistic compressor it may be advantageous to do so. The same equipment that is used for CARS experiments is used for SRG. The process involved is illustrated in Fig. 13. Rather than observe frequency mixing at the anti-Stokes frequency, gain of the Stokes wave is measured. The expected result for a broadband dye laser is shown in Fig. 13, i.e., gain in the high pressure medium caused by the pump beam ω_1 will modulate the Stokes laser spectrum as shown. The gain can then be determined by the local peak height relative to the pedestal, which is just the original Stokes laser profile. There are several advantages to stimulated Raman gain spectroscopy. The gain is proportional to Im $(\chi^{(3)})$ which has a resonant shape (Ref. 22); therefore there are no interference effects as with CARS and the background susceptibility has no effect. The integrated gain is directly proportional to the molecular species concentration. Furthermore there is no requirement for phase matching.

The estimates of Stokes laser gain factor, G indicate that with the high repetition frequency Nd:YAG lasers the gains are on the order of a few percent. The gain however can be increased by multiple passing the beams through the high pressure section with a light trapping cell (Refs. 36 and 37). With such a cell 10 passes are easily obtained (20-50 passes are feasible) thereby increasing the gain an order of magnitude. Passing the beams many times through the small windows of the ballistic compressor is nontrivial. Alternatively time resolution could be sacrificed and one of the lower repetition, higher power Nd:YAG lasers could be used provided the optical breakdown threshold is not exceeded. In any event the gain measured in the test section should be referenced to another cell maintained at a known, high pressure to eliminate the effect of laser pulse-to-pulse fluctuations.

The detection system would be similar to the CARS detection system. The Stokes beam would be dispersed from the pump beam with a prism. The Stokes beam would have to be attenuated by taking the reflection off an uncoated flat plus passing it through neutral density filters in order to avoid saturating the OMA. The Stokes beam would then be dispersed and swept across the two dimensional array of the OMA II in the same manner as previously discussed for CARS measurements.

The choice between CARS and SRG is not clear cut. The lasers, and detection apparatus are identical, so that both techniques could be implemented, investigated and compared. Analysis of data is certainly easier with SRG. Although collisional narrowing must be accounted for with both techniques, in principle it is simpler for SRG. A multipass cell will be required for SRG but is not expensive for a modest number of passes. SRG would have definite advantages when the signal strength is high enough.

STIMULATED RAMAN GAIN SPECTROSCOPY

● MEASUREMENT APPROACH
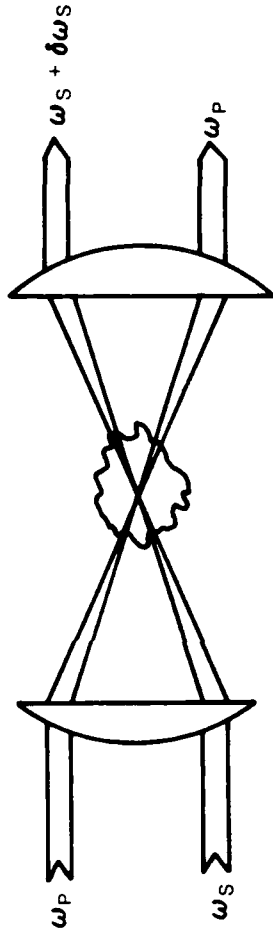
● ENERGY LEVEL DIAGRAM
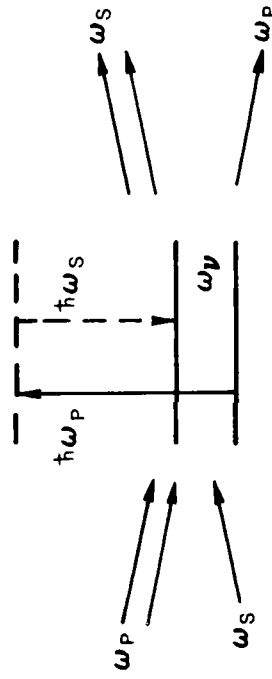
● SPECTRUM
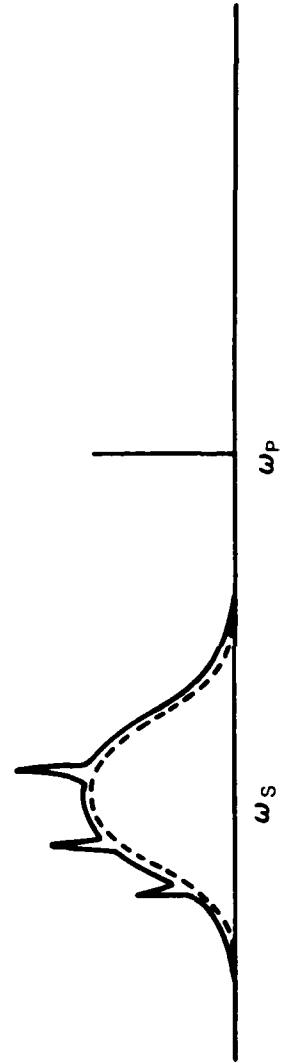
SECTION V

CONCLUSIONS

Estimates have been made of the performance of a CARS diagnostic system for
the AMMRC ballistic compressor. The high reptition rate Nd:YAG laser alone provides
adequate signal-to-noise ratios for time resolved measuements. The advantages of
using hydrogen as a thermometric species have been pointed out. Signal-to-noise
ratios have been calculated for representative compressor conditions. The SNR's
are reasonable at high H_2 concentration, with a tradeoff in repetition rate, or
effectively time resolution, expected to yield substantially improved performance.
To predict the SNR for lower concentrations requires a knowledge of foreign gas
broadening coefficients, which are largely unknown. At worst the SNR scales
in direct proportion to hydrogen concentration, limiting the SNR to 53 at 1000
atmospheres for a 5 kHz rep rate for 10 percent concentration. Population satura-
tion, stimulated Raman gain, and optical breakdown are not expected to pose limita-
tions on laser intensity and measurement SNR. Finally operation of the ballistic
compressor itself does not appear to pose insurmountable problems for CARS diagnos-
tics.

The possibility of using SRG with a multipass cell also has been raised as
a possibility. Either CARS or SRG could be implemented using identical equipment.

SECTION VI

REFERENCES

1. Nibler, J. W., W. M. Shaub, J. R. McDonald and A. B. Harvey: Coherent Anti-Stokes Raman Spectroscopy, in Vol. 6 <u>Vibrational Spectra and Structure</u>, J. R. Durig Ed., Elsevier, Amsterdam, 1977.

2. Eckbreth, A. C., P. A. Bonczyk and J. F. Verdieck: Laser Raman and Fluorescence Techniques for Practical Combustion Diagnostics. Appl. Spect. Rev., <u>13</u>, 15 (1978).

3. Druet, S., and J. P. Taran: Coherent Anti-Stokes Roman Spectroscopy, in <u>Chemical and Biological Applications of Lasers</u>, C. B. Moore, Ed., Academic Press, New York, 1979.

4. Nibler, J. W., and G. V. Knighten: Coherent Anit-Stokes Raman Spectroscopy, in <u>Raman Spectroscopy of Gases and Liquids</u>, A. Weber, Ed., Springer-Verlag, Berlin, 1979.

5. Roh, W. B., P. W. Schreiber and J. P. E. Taran: Single-Pulse Coherent Anit-Stokes Raman Scattering. Appl. Phys. Letts., <u>29</u>, 174 (1974).

6. Eckbreth, A. C.: BOXCARS: Crossed-beam Phase-Matched CARS Generation in Gases, Appl. Phys. Letts., <u>32</u>, 421 (1978).

7. Laufer, G., and R. B. Miles: Angularly Resolved Coherent Raman Spectroscopy (ARCS), Optics Commun. <u>28</u>, 250 (1979).

8. Marko, K. A., and L. Rimai: Space and Time-Resolved Coherent Anti-Stokes Raman Spectroscopy for Combustion Diagnostics, Optics Letters <u>4</u>, 211 (1979).

9. Hall, R. J.: CARS Spectra of Combustion Gases. Comb. Flame, Vol. 35, pp. 47-60, 1979.

10. Hall, R. J., J. A. Shirley and A. C. Eckbreth: Coherent Anti-Stokes Raman Spectroscopy: Spectra of Water Vapor in Flames, Optics Letters <u>4</u>, 87 (1979).

11. Dion, P., and A. D. May: Motional Narrowing and Other Effects in the Q Branch of HD, Can. J. Phys., <u>51</u>, 36 (1973).

REFERENCES (Cont'd)

12. DeWitt, R. N., A. B. Harvey, and W. M. Tolles: Theoretical Development of Third-Order Susceptibility as Related to Coherent Anti-Stokes Raman Spectroscopy (CARS), NRL Memorandum Report 3260, (1976).

13. Herzberg, G.: Molecular Spectra and Molecular Structure, I. Diatomic Molecules. D. Van Nostrand, Princeton, NJ (1945).

14. Allen, E. J., A. D. May, B. P. Stoicheff, J. C. Stryland and H. L. Welsh: Spectroscopy Research at the McLennan Physical Laboratories of the University of Toronto. Appl. Optics 6, 1597 (1967).

15. RCA Technical Manual PT-60, Phototubes and Photocells, Radio Corp. of America, 1963.

16. Dunn, M. H., and J. N. Ross: The Argon Ion Laser, Prog. Quant. Electron 4, 223 (1976)

17. Profit, W. and J. Ryan, Coherent, Palo Alto, Calif., private communication.

18. Cramer, L. Spectra Physics, Mountain View, Calif., private communication.

19. Koechner, W.: Solid-State Laser Engineering, Springer-Verlag, New York, (1976).

20. Yariv, A., Quantum Electronics, 2nd Ed., J. Wiley, New York, NY, (1967).

21. Popper, R, Enmark Associates (representative for Control Laser Corporation; Orlando, Fla.), private communication.

22. Maier, M.: Applications of Stimulated Raman Scattering. Appl. Phys. 11, 209 (1976).

23. Lalos, G. T., and G. L. Hammond: The Ballistic Compression and High Temperature Properties of Dense Gases. Chap. 25 in Experimental Thermodynamics IUPAC Butterworths (1975).

24. Regnier, P. R., F. Moya and J. P. E. Taran: Gas Concentration Measurement by Coherent Raman Anti-Stokes Scattering. AIAA J., 12, 826 (1974).

25. Smith, D. C., and R. G. Meyerand, Jr.: Laser Radiation Induced Gas Breakdown, Chapter 11 in Principles of Laser Plasmas, G. Beketi, Ed., Wiley Interscience, New York, 1974.

REFERENCES (Cont'd)

26. Lencioni, D. E.; Laser-Induced Air Breakdown for 1.06 μm Radiation. Appl. Phys. Letts. 25, 15 (1974).

27. Smith, D. C., and R. T. Brown: Aerosol-Induced Air Breakdown With CO_2 Laser Radiation. J. Appl. Phys. 46, 1146 (1975).

28. Switzer, G. L., C. G. Meyers, Jr., W. B. Roh and P. W. Schreiber: Gas Breakdown Thresholds in Flames Induced by Ruby Laser, AIAA J. 16, 766 (1978).

29. EG&G Princeton Applied Research; Princeton, NJ.

30. Galeener, F. L., J. C. Mikkelsen, R. H. Geils and W. J. Mosby: The Relative Raman Cross Sections of Vitreous SiO_2, GeO_2, B_2O_3 and P_2O_5. Appl. Phys. Lett. 32, 34 (1978).

31. Levenson, M. C.: Feasibility of Measuring the Nonlinear Index of Refraction by Third-Order Frequency Mixing. IEEE J. Quant. Elect. QE-1 110 (1974).

32. Straat, H. W.: A Marginal Ray Trace Program for the TI-59 Calculator. Optical Spectra 12, 68 (Aug. 1978).

33. Hall, R. J.: Theory of High Pressure CARS Spectra, UTRC Report No. UTRC-79-127 (1979).

34. Owyoung, A., Sandia Laboratory, Albuquerque, NM, private communications.

35. May, A. D., J. C. Stryland, and G. Varghese: Collisional Narrowing of the Vibrational Raman Band of Nitrogen and Carbon Monoxide. Can. J. Phys., 45, 2331 (1970).

36. Hartley, D. L., and R. A. Hill: A Highly Efficient Light-Trapping Cell for Raman Scattering Measurements. J. Appl. Phys. 43, 4134 (1972).

37. Owyoung, A.: Sensitivity Limitations for CW Stimulated Raman Spectroscopy. Optics Comm. 22, 323 (1977).

DISTRIBUTION LIST

No. of Copies	To
1	Office of the Under Secretary of Defense for Research and Engineering, The Pentagon, Washington, D. C. 20301
12	Commander, Defense Technical Information Center, Cameron Station, Building 5, 5010 Duke Street, Alexandria, Virginia 22314
1	Metals and Ceramics Information Center, Battelle Columbus Laboratories, 505 King Avenue, Columbus, Ohio 43201

Deputy Chief of Staff, Research, Development, and Acquisition,
Headquarters, Department of the Army, Washington, D. C. 20310
1 ATTN: DAMA-ARZ

Commander, Army Research Office, P. O. Box 12211, Research
Triangle Park, North Carolina 27709
2 ATTN: Information Processing Office

Commander, U. S. Army Materiel Development and Readiness Command,
5001 Eisenhower Avenue, Alexandria, Virginia 22333
1 ATTN: DRCLDC, Mr. R. Zentner

Commander, U. S. Army Materiel Systems Analysis Activity,
Aberdeen Proving Ground, Maryland 21005
1 ATTN: DRXSY-MP, H. Cohen

Commander, U. S. Army Electronics Research and Development Command,
Fort Monmouth, New Jersey 07703
1 ATTN: DELSD-L
1   DELSD-E

Commander, U. S. Army Missile Command, Redstone Arsenal, Alabama 35809
1 ATTN: Technical Library

Commander, U. S. Army Armament Research and Development Command,
Dover, New Jersey 07801
2 ATTN: Technical Library
1   DRDAR-SCM, J. D. Corrie
1   DRDAR-LCA, Mr. Harry E. Pebly, Jr., PLASTEC, Director

Commander, U. S. Army Foreign Science and Technology Center,
220 7th Street, N. E., Charlottesville, Virginia 22901
1 ATTN: Military Tech, Mr. Marley

Naval Research Laboratory, Washington, D. C. 20375
1 ATTN: Dr. J. M. Krafft - Code 8430

No. of Copies	To
	Chief of Naval Research, Arlington, Virginia 22217
1	ATTN: Code 471
	Air Force Materials Laboratory, Wright-Patterson Air Force Base, Ohio 45433
2	ATTN: AFML/MXE/E. Morrissey
1	AFML/LC
1	AFML/LLP/D. M. Forney, Jr.
1	AFML/MBC/Mr. Stanley Schulman
	National Aeronautics and Space Administration, Washington, D. C. 20546
1	ATTN: Mr. B. G. Achhammer
1	Mr. G. C. Deutsch - Code RW
	National Aeronautics and Space Administration, Marshall Space Flight Center, Huntsville, Alabama 35812
1	ATTN: R. J. Schwinghammer, EH01, Dir, M&P Lab
1	Mr. W. A. Wilson, EH41, Bldg. 4612
1	Mechanical Properties Data Center, Belfour Stulen Inc., 13917 W. Bay Shore Drive, Traverse City, Michigan 49684
1	Dr. Robert S. Shane, Shane Associates, Inc., 7821 Carrleigh Parkway, Springfield, Virginia 22152
	Director, Army Materials and Mechanics Research Center, Watertown, Massachusetts 02172
2	ATTN: DRXMR-PL
1	DRXMR-PR
1	DRXMR-PD
1	DRXMR-AP
5	DRXMR-RA, Dr. K. Tauer

AD

Army Mechanics and Materials Research Center
Watertown, Massachusetts 02172
CONCEPTUAL DESIGN STUDY FOR COHERENT
ANTI-STOKES RAMAN SPECTROSCOPY (CARS)
DIAGNOSTICS IN THE AMMRC BALLISTIC COMPRESSOR
FACILITY -
John A. Shirley and Robert J. Hall, United
Technologies Research Center, E. Hartford, Conn. 06108

Technical Report AMMRC TR80-7, April 1980, 48 pp-
illus-tables, contract DAAG46-79-0060
D/A Project 1L161102AH42, AMCMS Code
Final Report, July 1979-Nov. 1979

KEY WORDS

Raman Spectroscopy
CARS
Gas Temperatures
Rapid determination

A conceptual design of a diagnostic system using coherent anti-Stokes Raman spectroscopy (CARS)
to determine time resolved temperature and species concentrations in the Army Mechanics and
Materials Research Center ballistic compressor has been formulated. Performance calculations
have been carried out for hydrogen which is an ideal diagnostic species for this application.
Results are also presented of computer code calculations of collision narrowed spectra of
nitrogen. Several pump laser systems were compared, and a high repetition frequency Nd:YAG
laser was determined to be superior. Population saturation, stimulated Raman gain, and optical
breakdown are not expected to pose severe limitations on laser intensity or measurement signal-
to-noise ratios. Consideration is given to problems pertinent to operation of the ballistic
compressor including compressor recoil, window deflections and generation of CARS from the test
section windows. Finally the possibility of using pulsed stimulated Raman gain spectroscopy (SRGS)
as an alternative to CARS at the high densities typical of the ballistic compressor has been identi-
fied. SRGS appears to offer adequate measurement ability and possesses certain advantage over CARS.